Dear Dr. Hoppema,

Thank you very much for handling our manuscript. Following the reviewer's comment, we have revised the manuscript. Below, the reviewers' comments are indicated in black text and our responses are indicated in red text. Line numbers below refer to the tracked-changes version of the manuscript, although in the author comments in the interactive discussion, line numbers refer to the revised, non-tracked-changes version manuscript. In addition to the comments from the reviewers, we received some comments from researchers of the National Oceanographic Centre, UK., personally. We have revised the manuscript taking into account their comments as well. Their comments and our replies are also included below.

Reply to referee #1:

Thank you very much for invaluable comments and suggestions on our original manuscript. According to the comments, we have revised the manuscript. In addition, following the comment we received personally from the National Oceanographic Centre, UK. (For their comments and our reply, see Pages 15–24), we have combined Section 3.2 and 3.3 in the original manuscript and reorganized. We think the revised manuscript is now more readable. We hope that the revised manuscript meets your approval and will be more suitable for publication in the journal.

Reply to comments:

(Referee #1) "The authors present an interesting work to compare the relationship of air-sea carbon fluxes to ENSO in the equatorial Pacific simulated by the two earth system models with assimilation and without assimilation, which are developed by the same institute. What's more interesting in this paper is that the old earth system model with assimilation generated an incorrect upwelling during the El Nino period, which led to a great problem in the simulation of carbon fluxes, but the new earth system model did not. Although this work has not made much contribution to the study of the response mechanism of carbon fluxes to ENSO in the equatorial Pacific, it will be very helpful to the people who are interested in assimilation or the model development, especially to those who are interested in the simulation of the carbon cycle process in the equatorial Pacific, if we can find out why the old and new models have different performances after the same assimilation method is added.

The content of the article fits within the scope of OS, but much work needs to be done before publication to refine the theme of the article, highlight key points, and give a more detailed discussion on the conclusions."

Thank you for taking the time to review the manuscript. We have revised the manuscript in accordance with the following comments. We will answer them point by point.

Major points:

1 Abstract Great changes are needed to reduce the description of the study significance and increase the discussion of the final result.

We have completely rewritten the abstract. First, the first two sentences in the abstract in the original manuscript have been removed for conciseness and clearness on the purpose of this study. We then have described in more detail what led to the failure of reproducing the observed anticorrelation between SST and CO2F in the eastern equatorial Pacific with the ESM with smaller-than-observed amplitude of ENSO.

2 Some descriptions need to be supplemented, such as the vertical range of assimilation. Are the temperature and salinity at the bottom of the mixed layer assimilated? That another content needs to be added is to compare the differences in the simulation of ENSO between the two models with assimilation and without assimilation, such as the periodicity and amplitude of ENSO.

In this study, the observed anomalies are assimilated into the ocean models at depths between the sea surface and 3000 m. We have rewritten Lines 257–258 of the revised manuscript as follows:

"In addition, the IAU was applied at depths between the sea surface and 3000 m, with the values of $\tau = 1$ day and $\alpha = 0.025$ (Tatebe et al., 2012)."

The original manuscript did not clearly state that we used "anomaly assimilation". We have added the following sentences in Lines 254–257 in the revised manuscript:

"For $X^a(0)$ and $X(0)$, we used anomalies from monthly mean climatology during 1961–2000 in observations and models, respectively. Such a scheme often called 'anomaly assimilation' or 'anomaly initialization' is used in many previous studies (e.g., Smith et al., 2007; Keenlyside et al., 2008; Pohlmann et al., 2009; Li et al., 2016, 2019; Sospedra-Alfonso and Boer, 2020)."

We have added Table 2 showing intensities and periods of ENSO for NEW, OLD, and

observations in the revised manuscript. The discussion on the intensities (periods) of ENSO has been added in Lines 373–375 (612–616) in the revised manuscript. The ENSO intensities and periods for NEW-assim and OLD-assim are the same as the observed values because of data assimilation.

3 In the old model with and without assimilation, the response of 10-m wind speed over the sea surface to NINO3-SST does not change significantly, but the response of sea water vertical velocity to NINO3-SST changes greatly (Figure 4). Dose the meridional wind change significantly?

In OLD-assim, the warming due to data assimilation procedure during El Niño periods reduces density at the depth of the thermocline in the eastern equatorial Pacific, leading to enhancement of upward vertical velocity. The patterns of zonal and meridional wind speed variation in OLD and OLD-assim are similar. To describe the mechanism causing vertical velocity anomalies more clearly, we have added Figure S3 as a supplement and modified Lines 601–605 in the revised manuscript as follows:
"The wind feedback in OLD-assim is 0.48 m s^{-1} K^{-1} (Table 3), which is the same as in OLD, and the map of the wind speed anomalies shows a similar pattern to that of the OLD (Figure S3e–h); however, the warming due to data assimilation procedure during El Niño periods reduces density, leading to low-pressure anomalies. This results in anomalous cyclonic circulation and convergence, and thus enhancement of upward vertical velocity at the depth of the thermocline (Figure 5d)"

4 Line 196, "howerver, the strong heating causes upwelling of DIC rich waters in the subsurface layers (Figure 6b)." Why does this strong heating occur? Is the simulated value of sea water temperature in the old model during the El Nino period lower than the data used for the assimilation? Please discuss in detail the reasons for the abnormal upwelling during the El Nino period in the old model with assimilation.

In this study, the observed anomalies are assimilated into the ocean models at depths between the sea surface and 3000 m (see Reply to Major points 2). In OLD, the temperature variations in the eastern equatorial Pacific is smaller than observed (Figure 3b and 3c), so that the correction term on the governing equation of the ocean temperature, which is introduced in the data assimilation procedure, forces to raise the equatorial water temperature during El Niño

periods in order to realize observed temperature variations. To clarify this process, we have modified Lines 598–601 in the revised manuscript as follows:

"In OLD, the temperature variations associated with ENSO at the depth of the thermocline in the eastern equatorial Pacific is smaller than observed (see Figure 3b and 3c), so that the correction term forces to raise the equatorial water temperature by 0.16×10^{-6} °C s^{-1} during El Niño periods in order to realize observed temperature variations (Figure 5b). "

In order to describe the process in which warming causes the enhancement of upward vertical velocity more clearly, we have rewritten Lines 603–605 as follows:

"the warming due to data assimilation procedure during El Niño periods reduces density, leading to low-pressure anomalies. This results in anomalous cyclonic circulation and convergence, and thus enhancement of upward vertical velocity at the depth of the thermocline (Figure 5d)."

5 After assimilation is added to the new earth system model, the response of upwelling anomalies to NINO3- SST is weakened (comparison of Fig. 6 with Fig. 8). This change in the response is actually similar to that in the old model. Does this mean that the current assimilation method is not suitable to the earth system model?

This study points out that, before discussing the assimilation methods, the performance of the model itself needs to be improved. We think that the reproduction of the observed anticorrelated relationship between SST and CO2F in the equatorial Pacific in NEW-assim indicates the usefulness of the MIROC-ES2L and the data assimilation method we used in this study.

However, we have to admit that MIROC-ES2L and the data assimilation method we used is not perfect. As the referee #1 pointed out, the assimilation scheme modifies the distribution of vertical velocity. At 140W, the upward vertical velocity anomaly during El Niño periods was -7×10^{-6} m/s in New, but it changed to about -5×10^{-6} m/s in the NEW-assim. The change in the upward vertical velocity from NEW to NEW-assim may be due to the fact that the ENSO intensity is stronger and the period is longer than in the observations, and response of vertical velocity in ENSO is still distorted by the temperature analysis increment in NEW-assim. To point out that the response of vertical velocity in ENSO is still distorted by the temperature analysis increment in NEW-assim, we have added the following sentences in Lines 611–616:

"As already discussed, the intensity of ENSO in NEW is slightly stronger than observed (Table 2). In addition, the period of ENSO, which is defined as the peak of the power spectrum of one-year running mean NINO-SST, is 5.0 years in NEW, which is longer than 3.5 years of observations (see Table 2). Because the ENSO characteristics in NEW are somewhat

inconsistent with observations, model nature, namely responses of vertical velocity and DIC concentration in ENSO, are still distorted by the temperature analysis increment even in NEW-assim. This indicates that further model improvements are needed."
We think that the further development of ESM and the use of more advanced assimilation methods may improve the performance of the model. Further investigation is required to identify the best suitable method and why.

Minor points:

1 Line 119, "three ensemble members". How were the ensemble experiments conducted? Were the initial fields of these experiments different?

Both of NEW and OLD are the exactly same as the historical simulations designated by CMIP6 and CMIP5 protocols, respectively, and they have three ensemble members which are bifurcated from arbitrary years of the corresponding preindustrial control simulations. NEW-assim and OLD-assim are bifurcated from NEW and OLD at the year 1946, respectively. We have added the following sentences in Lines 262–265 in the revised manuscript:
"Both of NEW and OLD are the exactly same as the historical simulations designated by CMIP5 and CMIP6 protocols, respectively, and they have three ensemble members which are bifurcated from arbitrary years of the corresponding preindustrial control simulations. The ocean data assimilation experiments, NEW-assim and OLD-assim, are bifurcated from NEW and OLD at the year 1946, respectively, and they are integrated up to the year 2005."

2 The statement of Line 149-151 is error. $(\partial pCO2/\partial T)\Delta T$ is not the term of changing the solubility of CO2.

The phrase "in CO2 solubility" in Lines 149–151 in the original manuscript has been removed.

3 How was the "temperature increment" calculated?

The phrase "temperature increment" in the original manuscript has been changed to "temperature analysis increment" in the revised manuscript. The method for calculating the temperature analysis increment is described in Sect. 2.1 in the revised manuscript, but here is a brief introduction. The analysis increment during the analysis interval from $t = 0$ to $t = \tau$ is calculated from $\Delta X^a = X^a(0) - X(0)$, where $X^a(0)$ is the analysis and $X(0)$ is the model first guess

at $t = 0$; this term is held constant during the analysis interval $\tau = 1$ d. The monthly objective analysis data of ocean temperature and salinity (Ishii and Kimoto, 2009) were interpolated linearly to form daily analysis data, X^a.

4 Line 236-238, “The correlation between SST and CO2F in the equatorial Pacific is consistently represented only in the case where the ocean temperature and salinity observations are assimilated into NEW.” This statement is ambiguous, because both OLD and NEW experiments can produce the relationship between the SST and CO2F.

We realized that the first paragraph of Discussion and Summary section, as in abstract (see Reply to Major points 1), should be a concise statement of what we found in the study. We have removed the description of the background from the first paragraph of Discussion and Summary in the original manuscript and rewritten it so that there was no ambiguity. The relevant sentence has been changed to:
”In the case where the ocean temperature and salinity observations were assimilated into the other ESM with rather realistic ENSO representation, anticorrelated relationship between SST and CO2F was reproduced.” (Lines 652–653)

5 Overall, the manuscript needs to be improved, including some language errors. ”

We have reviewed the entire manuscript and revised it in accordance with the comments. Thank you again for your comments.

Reply to referee #2:

Thank you very much for invaluable comments and suggestions on our original manuscript. Following the comments, we have revised the manuscript. In addition, following the comment we received personally from the National Oceanographic Centre, UK. (For their comments and our reply, see Pages 15–24), we have combined Section 3.2 and 3.3 in the original manuscript and reorganized. We think the revised manuscript is now more readable. We hope that the revised manuscript meets your approval and will be suitable for publication in the journal.

Reply to comments:

(Referee #2) "This paper describes the benefits of advanced data assimilation method in advanced CMIP6-class climate model compared to CMIP5 model. The model results and their mechanisms have been well described in this manuscript. I would recommend this paper is acceptable in this Ocean Science Journal with some support analysis based on comparison using observations to verify the assimilation skills, which could be much elevating the values of this paper.

Thank you very much for your comments.

L52. Can we discard the biological pump on the results, especially in the La Nina states? Author represented NINO3-CO2F correlation coefficients, which means both El Nino and La Nina events. As we know, decreasing the phytoplankton in El Nino event could affect the CO2F variability modulated by DIC solely but I wonder whether the strong positive bloom in La Nina event could absorb the CO2 into the ocean. If then, the better performance of the phytoplankton assimilation skill can be a key to elevate the better CO2F skill. Composite analysis between CO2F at El Nino and La Nina and taking difference of them to see the asymmetry would elevate the biological influence on CO2F in this model. If then, you may provide supporting figures of chlorophyll skills in this model using satellite-derived chlorophyll concentration using such as ESA-CCI (https://esa-oceancolour-cci.org) or GlobalColour in Hermes (http://hermes.acri.fr).

Thank you for your suggestion. We here examine the effect of the biological pump on CO_2 flux in the equatorial Pacific. First of all, we investigated whether NEW-assim captures the historical variations in the bloom magnitude associated with ENSO. Figure R1a shows the timeseries of simulated surface chlorophyll concentration anomalies averaged over the Niño3

region (hereafter NINO3-Chla) and NINO3-SST anomalies in NEW-assim. NINO3-Chla anomalies derived from the observational dataset Ocean Colour Climate Change Initiative (OC-CCI) dataset, Version 4.2, European Space Agency, is also shown. Here, monthly anomalies were calculated with respect to the 1998–2005 monthly mean climatology because OC-CCI dataset is only available since September 1997. The results of NEW-assim shows that NINO3-Chla increased during La Niña, and the correlation coefficient between NEW-assim and the observed values was estimated to be 0.60, indicating that NEW-assim is able to capture the variations in primary production associated with ENSO. It should be noted here that the variation of NEW-assim is larger than the variation of the observed values. Since NEW-assim captures the historical variations in the bloom magnitude associated with ENSO, we next calculate the average of NINO3-CO2F for El Niño, La Niña, and others (neutral), respectively (Figure R1b). Here, following Japan Meteorological Agency, "El Niño event" is defined as a phenomenon in which the five-month running mean of the NINO3-SST anomaly exceeds +0.5°C for six consecutive months or more, and "La Niña event" as a phenomenon in which the five-month running mean of the NINO3-SST anomaly is below −0.5°C for six consecutive months or more (Figure R1a). The anomaly of NINO3-CO2F averaged during El Niño periods is −0.43 $\mu gCO_2\ m^{-2}\ s^{-1}$, and that averaged during La Niña periods is 0.36 $\mu gCO_2\ m^{-2}\ s^{-1}$. The absolute value of NINO3-CO2F anomaly averaged during La Niña periods is 15% smaller than that of El Niño periods, which can be explained by the biological pumps during La Niña periods. However, the standard error bar of NINO3-CO2F during La Niña periods overlaps that during El Niño periods, so that the difference in NINO3-CO2F is not significant and we did not include these results in the revised manuscript. Further studies are needed to quantify the effect of biological pump.

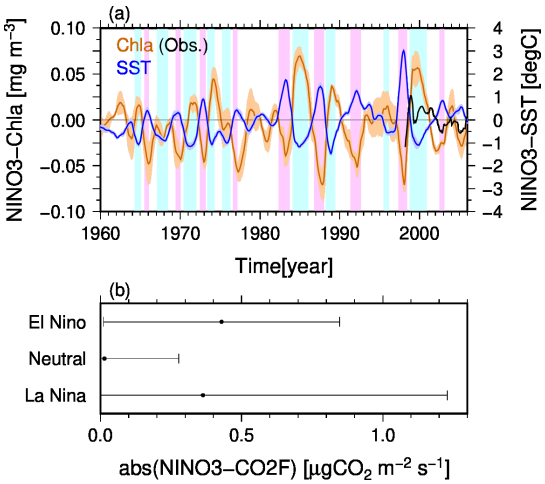

Figure R1. (a) Timeseries of the detrended NINO3-Chla for NEW-assim (orange line) and observations

(black). The blue line is the timeseries of the detrended NINO3-SST anomalies in NEW-assim. Values plotted are the one-year running mean and shading shows the ensemble spread (1σ). The El Niño and La Niña periods is indicated by light magenta and light cyan, respectively. (b) Absolute values of monthly mean NINO3-CO2F anomalies averaged over El Niño, La Niña, and other (neutral) periods, respectively, during the period from 1960 to 2005 simulated with NEW-assim. Error bars indicate the standard deviations of monthly mean NINO3-CO2F anomalies. Note that they are not the standard deviations of the absolute values of monthly mean NINO3-CO2F.

L142. What about observational skills in the region for CO2F associated with ENSO compared to NEW-assim skill -0.41? This can be depending on the definitions of regional and temporal scales but as you cited Dong et al (2016) represents above 0.6 skills in many CMIP5-class model (it seems like opposite sign for CO2F). Of course they do not have assimilation but do you think the ENSO-CO2F skill is generated by some limitations coming from assimilation? Otherwise you may add comparison between OLD and NEW model correlation (or regression) skill of ENSO-CO2F without assimilation (freerun) to argue this issue as a table likewise arranging skills of OLD, OLD-assim, NEW, NEW-assim and with skill of available SST reanalysis and psudo observation data of CO2 flux at least single observation dataset such as using Landschutzer et al 2016 (link: https://www.nodc.noaa.gov/ocads/oceans/SPCO2_1982_2015_ETH_SOM_FFN.html), opened to public or data-based estimates of carbon cycle variability (http://www.bgc-jena.mpg.de/CarboScope/?ID=oc), which is needed by personal contact to access. If then, you may add some figures and discussions in chapter 3.1 for comparison of ENSO-related CO2F skills between in observation, OLD, and NEW model in spatial and temporal scales. If the results are significant, this could be providing the most benefit in this paper and persuading rest of results being reasonable. According to this, you may see some figures and references in Hongmei Li et al. 2019 as you cited."

Thank you for your suggestion. In order to discuss the correlation coefficients between CO2F and SST in each experiment, we have added Table 1 in the revised manuscript. We have recalculated the correlation coefficients between CO2F and SST in NEW-assim, and it was estimated to be –0.50. The absolute value of the correlation coefficient in NEW-assim is less than the absolute value of the correlation coefficient of NEW (–0.85). This is because model nature are somewhat distorted by the temperature analysis increment even in NEW-assim. In the revised manuscript, we have added the following sentence in Lines 614−616:
"Because the ENSO characteristics in NEW are not perfectly consistent with observations, model nature, namely responses of vertical velocity and DIC concentration in ENSO, are still

distorted by the temperature analysis increment even in NEW-assim. This indicates that further model improvements are needed."

To compare the maps for the correlation coefficients between CO2F from SOM-FFN and that from the NEW-assim or from OLD-assim, we have added the new figures in the revised manuscript (Figure 1a and 1c). CO2F in NEW-assim (Figure 1a) is positively correlated with SOM-FFN in the equatorial Pacific. On the other hand, CO2F in OLD-assim shows a negative correlation with SOM-FFN there. In Lines 320–326 in the revised manuscript, we have added the description of these figures. The description on SOM-FFN has been added in Sect. 2.3 in the revised manuscript.

Reply to referee #3:

Thank you very much for invaluable comments and suggestions on our original manuscript. We would like to answer the questions given by the referee and to describe how we have revised our manuscript point by point. In addition, following the comment we received personally from the National Oceanographic Centre, UK. (For their comments and our reply, see Pages 15–24), we have combined Section 3.2 and 3.3 in the original manuscript and reorganized. We think the revised manuscript is now more readable. We hope that the revised manuscript meets your approval and will be more suitable for publication in the journal.

Reply to General comments:

(Referee #3) "This study is an important contribution for understanding ENSO and carbon fluxes variations in the equatorial Pacific. The authors have investigated the processes in regulating the relationship between ENSO and carbon fluxes in assimilations with nudging ocean temperature and salinity based on two MIROC models, i.e., OLD MIROC-ESM and NEW MIROC-ES2L. They demonstrated that the ability of model in producing correct amplitude of ENSO is crucial for reproduction of the air-sea CO2 flux variations in coherence with ENSO. Both the storyline and the writing are clear. However, there are still some unclear aspects listed as below, I would expect the authors further clarify them and improve the manuscript.

Thank you very much for your comments. We have reviewed the entire manuscript and revised it in accordance with the comments.

1. It is exciting to see the NEW model shows promising results of the anticorrelation between ENSO and air-sea CO2 flux, which the OLD model couldn't capture well especially the magnitude of ENSO. As revealed by Dong et al. (2016), most CMIP5 models could not capture the relationship right. It would be helpful to have some discussion on which key model developments do improve the representation of ENSO magnitude in the NEW model? A paragraph of discussion on this will provide advices for other modeling centers.

The important model improvements in MIROC-ES2L was not stated in the original manuscript. We have added the description on it in Lines 376–454 in the revised manuscript. In brief, one is implementation of an updated plume model for cumulus convection with multiple cloud types

where lateral entrainment rate varies vertically depending on the surrounding environment. The other is reduction of numerical diffusion by introducing highly-accurate tracer advection scheme in the ocean and by increasing vertical resolutions.

2. ENSO is an air-sea coupled system, it involves both ocean and atmosphere processes. In this study, both OLD-assim and NEW-assim only nudge ocean temperature and salinity, the atmosphere ran freely without any data nudging. I have couple of questions here: i) Does the IAU apply to every ocean level including the ocean surface? ii) How is the atmosphere part for instance winds treated? As the ocean part has strong nudging, the atmosphere should be adjusted accordingly, the mismatch of ocean and atmosphere would cause some spurious circulation. iii) Why is this spurious upwelling only found in the OLD-assim? iv) Is the spurious upwelling obvious in the climatological mean state in OLD-assim comparing with the OLD? A comparison of climatology in the nudged data and the model free runs will help understand this point. v) Would a different assimilation method, e.g., including atmospheric circulation nudging, end up with a different conclusion?

i) In this study, the observed temperature and salinity are assimilated into the ocean models at depths between the sea surface and 3000 m. To state this, we have rewritten Lines 257–258 in the revised manuscript as follows:
”In addition, the IAU was applied at depths between the sea surface and 3000 m, with the values of $\tau = 1$ day and $\alpha = 0.025$ (Tatebe et al., 2012).”

ii) In the atmosphere, data assimilation is not used. To clarify this, we have added the following sentence in Line 261 in the revised manuscript:
“Also, any atmospheric observations/reanalysis are not applied.”
The ocean temperature and salinity observations were assimilated into ESMs and the atmosphere responds to them.

iii) Here, we describe the anomalies during El Niño periods, while the opposite applies during La Niña periods. In OLD, the ENSO signal is weaker than the observation, so that the correction term on the governing equation of the ocean temperature forces to raise the equatorial water temperature in order to realize observed temperature variations. The warming due to data assimilation procedure reduces density, leading to enhancement of upward vertical velocity at the depth of thermocline. In NEW, on the other hand, because amplitudes of the equatorial temperature anomalies are larger than in OLD and are closer to observations, the correction term in NEW-assim arisen from

the assimilation procedure was kept small enough not to cause spurious enhancement of upward vertical velocity. To describe in more detail the mechanism by which upward vertical velocity in the equatorial Pacific in OLD-assim enhances during El Niño periods, we have rewritten Lines 598–605 in the revised manuscript as follows:

"In OLD, the temperature variations associated with ENSO at the depth of the thermocline in the eastern equatorial Pacific is smaller than observed (see Figure 3b and 3c), so that the correction term forces to raise the equatorial water temperature by 0.16 $\times 10^{-6}$ °C s^{-1} during El Niño periods in order to realize observed temperature variations (Figure 5b). The wind feedback in OLD-assim is 0.48 m s^{-1} K^{-1} (Table 3), which is the same as in OLD, and the map of the wind speed anomalies shows a similar pattern to that of the OLD (Figure S3e–h); however, the warming due to data assimilation procedure during El Niño periods reduces density, leading to low-pressure anomalies. This results in anomalous cyclonic circulation and convergence, and thus enhancement of upward vertical velocity at the depth of the thermocline (Figure 5d)."

iv) In this study, the observed temperature and salinity anomalies are assimilated into the ocean models at depths between the sea surface and 3000 m, which was not described in the original manuscript. Therefore, the climatological mean states of ocean temperature and salinity with assimilation are same with those without assimilation. In order to clarify that the observed anomalies are assimilated into the model in this study, we have added the following sentences in Lines 254–257:

"For $X^a(0)$ and $X(0)$, we used anomalies from monthly mean climatology during 1961–2000 in observations and models, respectively. Such a scheme often called 'anomaly assimilation' or 'anomaly initialization' is used in many previous studies (e.g., Smith et al., 2007; Keenlyside et al., 2008; Pohlmann et al., 2009; Li et al., 2016, 2019; Sospedra-Alfonso and Boer, 2020)."

v) Different assimilation techniques could make the model correlate better with the observations. Further investigation is required to identify the best suitable method and why. However, we think if the model itself does not perform well, the assimilation process leads to an unnatural circulation, as in OLD-assim in this study.

3. Line 32: "…warm by 1.5C within ~20 years…" -> "…warm by 1.5C within ~20 years relative to the preindustrial state"

Corrected. (Line 72 in the revised manuscript)

4. Line 87: "This remainder.." -> "The remainder. . ."

Corrected. (Line 134 in the revised manuscript)

5. Combining Fig. 5 and Fig. 7, Fig. 6 and Fig. 8 will help readers for the comparison of OLD and NEW.

Following the comment, Figures 5 and 7 (Figures 6 and 8) in the original manuscript have been combined into Figure 4 (Figure 5) in the revised manuscript.

6. Line 234-236: “In this research, the same simple data assimilation scheme is incorporated into two ESMs, OLD in which the ENSO amplitude is about half the observed value and NEW with improved reproducibility of ENSO.” Is this statement of ENSO amplitude based on the free runs of the two models? It would be helpful to add panels of ENSO amplitude in the free runs with OLD and NEW models in Fig. 1.

We have added Table 2 in the revised manuscript, that shows the intensity and period of ENSO in NEW, OLD, and observations. We have also added Figure S2 showing the timeseries of the detrended NINO3-SST and NINO3-CO2F anomalies simulated by one ensemble member in OLD and NEW and that derived from the observation.

7. Line 237: “. . .is consistently represented. . .” here needs to be rephrased to make it clearer, e.g., the anticorrelation relationship between SST and CO2F. ”

In order to state the results of this study more concisely and clearly in Discussion and Summary section, its first paragraph has been totally rewritten and the relevant sentence has been modified as follows:
”In the case where the ocean temperature and salinity observations were assimilated into the other ESM with rather realistic ENSO representation, anticorrelated relationship between SST and CO2F was reproduced.” (Lines 652–653)

Reply to comment from the National Oceanographic Centre, UK.:

Thank you very much for invaluable comments and suggestions on our original manuscript. According to the comments, we have revised the manuscript. Here, we copied all your comments and answered to all your comments point by point using red font.

Reply to comments:

Main comments:

"Overall the study is important for the improvement of CMIP models and their ability to reproduce ENSO variability. The story is in good shape and we do not think new simulations are required. There are many points that need clarification and the wording needs tightening to avoid confusion in places. Some unanswered questions detailed below would improve this study and make it more widely applicable to other CMIP models. Overall, we think the study needs minor revisions.

Thank you for taking the time to review the manuscript. We have revised the manuscript in accordance with the following comments.

Minor Comments:

Abstract

Abstract needs to make it clearer what the research question - and answer is. Place the question clearly, perhaps phrase lines 13-15 with question. It is important to communicate in the abstract that the OLD model does not reproduce observations (it is assumed the reader already knows this), and the newer models does. The final line of the abstract is vague and could be (tersly) summarised with "new model is better than old". What are the consequences of this? Where does this work lead and what are the immediate implications?

Thank you for your comments. Following the comments, we have completely rewritten the abstract. To more concisely and clearly state the purpose of this study, the first two sentences in the original manuscript have been removed. We then have described in more detail what led to the failure of reproducing the observed anticorrelation between SST and CO2F with the ESM with smaller-than-observed amplitude of ENSO, and pointed out that the performance of the model is important when initializing an ESM.

Introduction

Introduction is long and takes a while to get to the main problem with the CMIP5 model. The main point of the paper, discrepancy between the observations and MIROC-ESM for El Niño amplitude and associated CO_2 flux, should be identified in the first paragraph more clearly rather than the end of paragraph 4 (lines 52-54).

Thank you for your advice. We have totally rewritten and shortened Introduction section in the revised manuscript. The main point of this manuscript described in fourth paragraph in the original manuscript has been moved to the first paragraph in the revised manuscript.

Lines 64-72, do we need the history of data assimilation in climate models to understand this paper?

We have removed the description of the history of data assimilation in climate models in the revised manuscript.

Lines 76-89, the last paragraph of the introduction should specify the question this paper will answer and set out the structure of the paper. The question is unclear. Instead, this paragraph has text about assimilation that should be in the methods section.

To clarify the purpose of this study in Introduction, we have moved some sentences describing ESMs and data assimilation methods in the original manuscript to Methods section in the revised manuscript.

Methods

Lines 99-104, the grid is very irregular was it interpolated? Is the model sensitive to grid (add ref)?

To the south of 63°N, spherical coordinates are used. Analyses of SST and CO_2 flux variations in the Niño3 region were performed using data from the original grid. In order to compare the air–sea CO2 flux of NEW-assim and OLD-assim to SOM-FFN dataset (Landschützer et al., 2016), model output is linearly interpolated into the SOM-FFN grid. To describe the interpolation, we have added the following sentence in Line 321 in the revised manuscript:

"The model output data were ensemble mean and linearly interpolated into the SOM-FFN grid."

Lines 99-104, the NEW model is deeper 5300 vs 6300. Is the model sensitive to this (add ref)? How is the model partitioned vertically? Sigma/z/hybrid coordinate? This is important since the stratification is a key part of your results.

The vertical level both in MIROC-ES2L and MIROC-ESM are in a hybrid σ–z coordinate system. We have added the phrase "in a hybrid σ–z coordinate system" in Line 149 and Line 152 in the revised manuscript, respectively. Since this study focuses on processes near the surface, we do not think the change in maximum depth has had much of an impact. Rather, increasing vertical resolution within the upper 500 m of depth has an impact. In order to describe the vertical resolution, we have added the following sentences in Lines 152–155 in the revised manuscript:
"The resolutions in MIROC-ES2L are higher than in MIROC-ESM. In particular, 31 (21) of the 62 (44) vertical layers in MIROC-ES2L (MIROC-ESM) are within the upper 500 m of depth. The increased number of vertical layers in MIROC-ES2L has been adopted in order to better represent the equatorial thermocline."

Line 118, the ensembles are only mentioned here. We need more detail. How are they different? Maybe use a table.

Both of NEW and OLD have three ensemble members which are bifurcated from arbitrary years of the corresponding preindustrial control simulations, and NEW-assim and OLD-assim are bifurcated from NEW and OLD, respectively. We have mentioned this by adding the following sentence in Lines 262–265 in the revised manuscript:
"Both of NEW and OLD are the exactly same as the historical simulations designated by CMIP6 and CMIP5 protocols, respectively, with three ensemble members for each which are bifurcated from arbitrary years of the corresponding preindustrial control simulations. The ocean data assimilation experiments, NEW-assim and OLD-assim, are bifurcated from NEW and OLD at the year 1946, respectively, and they are integrated up to the year 2005"

Line 133, equation is repeated in the text. Instead, define the variables here. For example, what is (∂pCO2/∂Alk)ΔAlk?

In the revised manuscript, we have defined $C(X)= (\partial pCO_2/\partial X)\Delta X$ (X=T, S, DIC, Alk), as

pCO_2 change due to the change in X, and stated that Res. in Eq (3), which includes second-order terms (Takahashi et al., 1993), was estimated so that the left-hand side and right-hand sides in Eq. (3) are equal. (Lines 302–304 in the revised manuscript).

Methods is missing description of the boxes NINO3 and NINO4 for someone not familiar with ENSO analysis. Why are the boxes picked? A map would be useful here.

We analyzed CO2F in Niño3 region because this region shows maximum variability region for CO2F. We have added the map for standard deviations of CO2F anomalies derived from observation-based CO2F dataset SOM-FFN (Landschützer et al., 2016) (Figure S1). In the revised manuscript, to clarify why we focus on CO2F in this region, we have added the following sentences in Lines 310–313:

"It shows significant interannual variation of CO2F in some specific regions such as the equatorial Pacific and high latitudes of both hemispheres (Figure S1). In Sect. 3, we focus on the CO2F in the Niño3 region (5°S–5°N, 150°W–90°W) which shows notable variation of CO2F in the equatorial Pacific. This region is also the maximum variability region for SST (Gill, 1980)."

Niño4 region is the maximum variability zone for westerly wind. To show this, we have added the map for 10 m zonal and meridional wind anomalies (Figure S3), and added the following sentence in Line 460 in the revised manuscript.

"Niño4 region is the maximum variability region for the equatorial trade wind (Figure S3)."

We have added the boxes indicating Niño3 and Niño4 regions in Figure 1a and 1c in the revised manuscript.

Results 3.1

Terminology in results sections needs tightening up throughout. There are cases where increase and decrease are used when the positive and negative phase of ENSO should be referenced. More specific use of El Niño or La Niña would be helpful instead of ENSO signal.

The anomalies shown in Figures 2–5 show the ones during El Niño. Therefore, we have decided to discuss anomalies during El Niño from the climatic field in the revised manuscript. To make it clearer, we have added the following sentence in Line 356 in Section 3.1 in the revised manuscript:

"In the following, we describe the anomalies during El Niño periods, while the opposite applies during La Niña periods."

In addition, in order to describe more clearly our results, we have rewritten Sect. 3 entirely.

Line 149-156, this feels important but difficult to follow, please rephrase.

To more clearly describe the pCO2 change associated with the changes in DIC concentration and in temperature, we have rewritten Lines 149–156 in the original manuscript as follows:
"In NEW-assim, NEW, and OLD, pCO_2 decreases because the effect of the decrease in pCO_2 with decreasing DIC concentrations is larger than that of the increase in pCO_2 with warming (Figure 2). In OLD-assim, however, the effect of the increase in pCO_2 with warming is larger than that of OLD, and the decrease in pCO_2 with decreasing DIC concentrations is smaller than that of OLD, resulting in an increase in pCO_2." (Lines 357–360 in the revised manuscript)

Results 3.2

Line 179-180, this is confusing, enhanced SST anomaly during both positive and negative phases of ENSO?

In the revised manuscript, Sections 3.2 and 3.3 in the original manuscript have been combined into one and reorganized. (See reply to comments on Sect. 3.3) We have moved the description of the vertical velocity feedback in Lines 179–180 in the original manuscript to Line 594 in the revised manuscript. To make it clear that the positive value of vertical velocity feedback indicates the enhancement of upward vertical velocity during El Niño periods, we have rewritten Lines 606–608 in the revised manuscript as follows:
"The positive value of vertical velocity feedback indicates the enhancement of upward vertical velocity at the depth of the thermocline during El Niño periods, which is inconsistent with observations."
The opposite applies during La Niña periods. (Line 356 in the revised manuscript)

Line 196, why does strong heating cause upwelling? This needs better explanation.

The correction term in the governing equation of the ocean temperature leads to decrease in density during El Niño periods, causing enhancement of upward vertical velocity. In order to more clearly state this, we have rewritten the manuscript as follows:
"the correction term forces to raise the equatorial water temperature by 0.16×10^{-6} °C s^{-1} during El Niño periods in order to realize observed temperature variations (Figure 5b)." (Lines

600–601)
“the warming due to data assimilation procedure during El Niño periods reduces density, leading to low-pressure anomalies. This results in anomalous cyclonic circulation and convergence, and thus enhancement of upward vertical velocity at the depth of the thermocline (Figure 5d).” (Lines 603–604).

Line 198, is it upwelling like in La Niña or is it upward mixing that means a smaller SST increase than would be expected for El Niño. The terminology needs to be tighter here. Please check phrasing like this throughout.

The positive value of vertical velocity feedback, discussed in Line 198 in the original manuscript, indicates the enhancement of the upward vertical velocity during El Niño periods, which in fact should not be occurring. To make it clear that the enhancement of upward vertical velocity was occurring during El Niño periods in OLD-assim, we have rewritten Lines 606–608 as follows:
“The positive value of vertical velocity feedback indicates the enhancement of upward vertical velocity at the depth of the thermocline during El Niño periods, which is inconsistent with observations.”
The opposite applies during La Niña periods. (Line 357 in the revised manuscript)
We have rewritten Sect. 3 to make it clear that enhancement of the upward vertical velocity is occurring during El Niño periods in OLD-assim.

Line 200, does OLD-assim, with the temperature amplitude increase, suggest a future forecasts of increasing global temperature using OLD would not give realistic results?
The OLD-assim results here need to be discussed especially carefully with the right terms. Be sure about whether it is giving a result that is the same direction but less strong or a result that is the opposite direction i.e. La Niña like conditions during expected El Niño.

In the Niño3 region in OLD-assim, an upward CO2F anomaly is found when the SST shows the positive anomaly, which is opposite to observations (Figure 1b in the revised manuscript). This is because, in MIROC-ESM, the amplitude of the seasonal–decadal scale variations in ocean temperature in the upper layer of the eastern equatorial Pacific is too much smaller than in observations (Figure 3), so that the correction term on the governing equation of the ocean temperature in OLD-assim forces to raise the equatorial water temperature in order to realize observed temperature variations, leading to an unnatural variations in the vertical velocity. We do not think that this result in OLD-assim means that the future projection by

MIROC-ESM, where things are determined by the physics in the model, are unrealistic. In fact, the estimates of global warming by MIROC-ESM is not extremely different compared to other models. Friedlingstein et al. (2014, J. Climate, doi:10.1175/JCLI-D-12-00579.1) evaluated the twenty-first-century global surface warming defined as the 2081–2100 average relative to the 1986–2005 average under the concentration-driven RCP8.5 scenario in CMIP5 models (their Table 3). In MIROC-ESM, the global surface warming was estimated to be 4.7 ℃, which is larger than the inter-model mean, 3.7 ℃, but same with HadGEM2-ES.

Results 3.3

Section 3.2 and 3.3 would be better merged and restructured.

Thank you for your advice. We have combined Section 3.2 and 3.3 in the original manuscript and reorganized.

Please explain what makes the stratification in NEW setup better than OLD? Could it be applied to other CMIP models than are bad at reproducing ENSO?

In Lines 376–454 in the revised manuscript, we have described the two updates in model configuration in MIROC-ES2L. One is implementation of an updated plume model for cumulus convection with multiple cloud types where lateral entrainment rate varies vertically depending on the surrounding environment. The other is reduction of numerical diffusion by introducing highly-accurate tracer advection scheme in the ocean and by increasing vertical resolutions. We think these can be applied to other ESMs.

Does the different vertical depth levels/max-depth between NEW and OLD affect stratification and DIC storage in deeper water column?

In order to better represent the equatorial thermocline, the increased number of vertical layers in MIROC-ES2L has been adopted. Please see the reply above one. As a result, the stratification and DIC storage in the deeper layers may also change. However, we have to note that these may have also been changed by changing the advection scheme (Lines 381–454) and the model spinup time (Watanabe S. et al., 2011; Hajima et al., 2020).

Discussion

Key messages could be that one model in CMIP is not enough since they can be biased by misrepresented processes such as ENSO.

As you pointed out, each ESM has a model-specific bias, so that in future predictions multiple models need to be used and evaluated along with the uncertainties. To state this, we have rewritten Lines 659–662 as follows:
"There are many ESMs where the ENSO characteristics and/or the SST-CO2F relationship are inconsistent with observations. Causes of this discrepancy should be addresses in future studies through, for example, multi-model analysis, and also process-based uncertainty estimation will be further required in initialized climate and carbon predictions as well as projections by ESMs."

Line 255-260, not really needed here, we suggest to remove.

We removed the last paragraph in the original manuscript.

Figures

Figure 1, add R-value. Add the same graphs for NEW and OLD without assimilation.

We have added R-values in Figure 1 in the revised manuscript. The timeseries of SST and air–sea CO_2 flux in the Niño3 region simulated with NEW and OLD has been added as Figure S2.

Figure 2, x-axis label is not attractive, we suggest the authors use a colour-coded legend for the whole figure.

To make it easier to compare the magnitude of each term in Eq. (3) in each experiment, we have redesigned Figure 2.

Do you really need Figure 4, maybe a table would be better or stating the values in the text.

The results, which were presented in Figure 4 in the original manuscript, are now shown in Table 3 in the revised manuscript.

Combine Figures 5 and 7 for side by side comparison. Same for 8 and 6.

We have combined Figures 5 and 7, and Figures 6 and 8 as suggested.

Clarify the meaning of Figures 5-8. What does the colour scale mean? How should it be interpreted? Do we need to know timescale of response? Is it all calculated on monthly data?

The variation shown in Figures 2–5 in the revised manuscript represents the one during El Niño periods, and the opposite applies during La Niña periods. To make it clearer, we have added the following sentence in Line 356 in the revised manuscript:
"In the following, we describe the anomalies during El Niño periods, while the opposite applies during La Niña periods."
In the original manuscript, it was not clearly stated that we were discussing the anomalies from the climatic state. To clarify the processes occurring in our experiments, we have totally rewritten Sect. 3 in the revised manuscript. For example, we have rewritten the description on the process occurring in NEW-assim as follows:
"The maximum absolute value of the equatorial temperature analysis increment in NEW-assim is found at 10–40 m depths in the eastern equatorial Pacific, shallower than the depth of the thermocline (Figure 5a)." (Lines 479–481)
"The westerly wind anomalies in NEW-assim leads to weakening of upward vertical velocity along the equator during El Niño periods (Figure 5c)." (Lines 483–484)
"The weakening of upward vertical velocity causes lesser supply of the DIC-rich subsurface water to the surface layer, leading to the decrease in surface DIC concentration (Figure 5e)." (Lines 597–598)

The period of ENSO in NEW is longer than observations, and the data assimilation procedure can partially distort the model nature even in NEW-assim, so that we think that reproducing the observed timescale of ENSO is important along with the intensity of ENSO. We have added Table 2 showing the intensities and periods of ENSO in NEW, OLD, and the observation, respectively, and the following sentences in Lines 612–616 in the revised manuscript:
"In addition, the period of ENSO, which is defined as the peak of the power spectrum of one-year running mean NINO-SST, is 5.0 years in NEW, which is longer than 3.5 years of observations (see Table 2). Because the ENSO characteristics in NEW are not perfectly consistent with observations, model nature, namely responses of vertical velocity and DIC concentration in ENSO, are still distorted by the temperature analysis increment even in NEW-assim."

Figures 3–5 in the revised manuscript were drawn using monthly mean anomalies. To

make it clear, the corresponding parts have been rewritten. For example, Lines 366–368 in the revised manuscript have been rewritten as follows:

“A cross section of the monthly ocean temperature anomalies regressed onto monthly mean NINO3-SST anomalies along the equatorial Pacific is presented in Figure 3, together with the climatological annual mean depths of the 18, 20, and 22 °C isotherms.”

Importance of El Niño reproducibility for reconstructing historical CO_2 flux variations in the equatorial Pacific

Michio Watanabe[1], Hiroaki Tatebe[1], Hiroshi Koyama[1], Tomohiro Hajima[1], Masahiro Watanabe[2], and Michio Kawamiya[1]

[1]Research Institute for Global Change, Japan Agency for Marine-Earth Science and Technology (JAMSTEC), 3173-25, Showa-machi, Kanazawa-ku, Yokohama, Kanagawa, 236-0001, Japan.
[2]Atmosphere and Ocean Research Institute, the University of Tokyo, 5-1-5, Kashiwanoha, Kashiwa, Chiba, 277-8564, Japan.

Correspondence to: Michio Watanabe (michiow@jamstec.go.jp)

Abstract. Based on a set of climate simulations utilizing two kinds of Earth System Models (ESMs) to which observed ocean hydrographic data are assimilated with an exactly same data assimilation procedure, we have clarified that successful simulation of observed historical air–sea CO_2 flux variations in the equatorial Pacific is tightly linked with the reproducibility of physical air–sea coupled processes. When an ESM with weaker amplitude of ENSO (El Niño Southern Oscillations) than observations was used for historical simulations with the ocean data assimilation, observed equatorial anticorrelated relationship between the sea surface temperature (SST) and air–sea CO_2 flux on seasonal–decadal timescales cannot be represented. The simulated CO_2 flux anomalies were upward (downward) during El Niño (La Niña) periods. The reason is that nonnegligible correction term on the governing equation of ocean temperature, which was added through the ocean data assimilation procedure, caused anomalously spurious equatorial upwelling (downwelling) during El Niño (La Niña) periods, which brought more (less) subsurface layer water rich in dissolved inorganic carbon (DIC) to the surface layer. This led to upward (downward) air–sea CO_2 flux anomalies during El Niño (La Niña) periods. On the other hand, such spurious vertical transport of DIC and resultant positively-correlated SST and air–sea CO_2 flux variations were not occurring in the historical simulations where the other ESM with rather realistic ENSO representation were used because the correction term arisen from the assimilation procedure was kept small enough not to disturb an anomalous advection-diffusion balance for the equatorial ocean temperature. Thus, the reproducibility of the tropical air–sea CO_2 flux variability with data assimilation can be significantly attributed to the reproducibility of ENSO in an ESM. Our results suggests that, when using data assimilation to initialize ESMs for carbon cycle predictions, the reproducibility of the internal climate variations in the model itself is of great importance.

削除: In the equatorial Pacific, air–sea CO_2 flux is known to fluctuate in response to inherent climate variability, predominantly the El Niño–Southern Oscillation (ENSO). For both investigation of the response of the carbon cycle to human-induced radiative perturbations and prediction of future global CO_2 concentrations, representation of the interannual fluctuation of CO_2 fluxes in Earth system models (ESMs) is essential. This study attempted to reproduce observed air–sea CO_2 flux fluctuations in the equatorial Pacific using two ESMs, to which observed ocean temperature and salinity data were assimilated. When observations were assimilated into an ESM whose inherent ENSO variability was weaker than observations, nonnegligible correction terms on the governing equation of the equatorial ocean temperature caused anomalously false equatorial upwelling during El Niño periods that brought water rich in dissolved inorganic carbon from the subsurface layer to the surface layer. Contrary to observation, this resulted in an unusual upward air–sea CO_2 flux anomaly that should not occur during El Niño periods. The absence of such unrealistic upwelling anomalies in the other ESM with the data assimilation reflects better representation of ENSO and the mean thermocline in this ESM without data assimilation. Our results demonstrate that adequate simulation of ENSO in an ESM is crucial for accurate reproduction of the variability in air–sea CO_2 flux and hence, in the carbon cycle

1 Introduction

Since the industrial revolution, vast quantities of greenhouse gases (e.g., CO_2) have been released into the atmosphere through human activities such as fossil fuel use and land use change. Increased atmospheric CO_2 concentration

leads to global warming, while both the oceanic and the terrestrial ecosystems absorb atmospheric CO_2 and are considered to work to relax the progress of the global warming (Sabine et al., 2004; Doney et al., 2009a, 2014; Le Quéré et al., 2009, 2010, 2016). Observation-based studies have reached consensus that significant interannual variability of the air–sea CO_2 flux (hereafter, CO2F) exists in some specific regions such as the equatorial Pacific and high latitudes of both hemispheres (e.g., Park et al., 2010; Valsala and Maksyutov, 2010; Landschützer et al., 2014; Rödenbeck et al., 2014), and the variation of CO2F associated with El Niño–Southern Oscillation (ENSO) in the equatorial Pacific has been highlighted in many previous observation-based and simulation-based studies (Keeling and Revelle, 1985; Feely et al., 1997, 1999; Jones et al., 2001; Obata and Kitamura, 2003; McKinley et al., 2004; Patra et al., 2005). When El Niño event occurs in the equatorial Pacific, dissolved inorganic carbon (DIC) concentration in the surface layer decreases due to lesser supply of the cold DIC-rich subsurface water to the surface layer than normal years because of weaker equatorial upwelling associated with weaker trade winds (Le Borgne et al., 2002; Feely et al., 2004; Doney et al., 2009a, 2009b). Correspondingly, CO2F is anomalously downward during El Niño, and vice-vasa during La Niña. Le Borgne et al. (2002) estimated that upwelling of DIC-rich subsurface water accounts for up to 70% of CO2F variation in the equatorial Pacific, while the other 30% is attributable to the variation of wind speed and biological processes. Accordingly, to estimate and predict variations of CO_2 uptake by the global ocean on timescales of several years, it would be informative to consider first the variations in the equatorial Pacific associated with ENSO.

The goal of the Paris Agreement is to restrict the rise of the global mean surface air temperature to well below 2 °C relative to the preindustrial level. If greenhouse gas emissions continue to increase at their current rate, Earth's surface will warm by 1.5 °C within ~20 years relative to the preindustrial state as reported in the fifth assessment report of the Intergovernmental Panel on Climate Change (IPCC, 2013). In this context, comprehensive understanding of the changes in the carbon cycle over previous years is essential for accurate predictions of the global carbon cycle, including natural variations, which will assist in evaluation of future CO_2 emission reductions (Kawamiya et al., 2019).

For future climate predictions, data assimilation procedures are incorporated into climate models in order to synchronize simulated climatic states in the model with observations, that is, initialization of climate models. By incorporating data assimilation procedures into Earth System Models (ESMs), it will be possible to reproduce and predict variations in biogeochemical properties (Brasseur et al., 2009; Tommasi et al., 2017a, 2017b; Park et al., 2018). This includes an assessment of the predictability of CO2F on decadal timescale for the global ocean (Li et al., 2016, 2019).

Focusing on CO2F fluctuations associated with ENSO in the equatorial Pacific, Dong et al. (2016) analyzed the results of the Earth system models (ESMs) that participated in the Coupled Model Intercomparison Project (CMIP) Phase 5 (CMIP5; Taylor et al., 2012), which contributed to the Fifth Assessment Report (AR5) of the Intergovernmental Panel on Climate Change (IPCC, 2013). They showed that only some ESMs could reproduce the observed anticorrelated relationship between SST and CO2F. This suggests that our understanding of ENSO and associated global carbon cycle variations are still insufficient. For reliable prediction of future CO_2 uptake on seasonal–decadal timescales, it is necessary to understand physical air–sea coupled process and associated carbon cycle variations in the equatorial Pacific.

削除: ; however,
削除: . Oceanic
削除: terrestrial CO_2 uptake constitutes one of the major processes governing the fluctuationare considered to work to relax the progress
削除: carbon cycle
削除:
The goal of the Paris Agreement is to restrict the rise of the global mean surface temperature to well below 2 °C relative to the preindustrial level. If greenhouse gas emissions continue to increase at their current rate, Earth's surface will warm by 1.5 °C within ~20 years (Intergovernmental Panel on Climate Change (IPCC), 2018). In this context, comprehensive understanding of the changes in the carbon cycle over previous years is essential for accurate prediction of the carbon cycle, including natural fluctuations, which will assist in evaluation of future CO_2 emission reductions (Kawamiya et al., 2019).
In the global climate, apart from the long-term warming trend associated with anthropogenic CO_2 emissions, there are inherent, self-excited, internal climate variations with seasonal–decadal timescales, e.g., El Niño–Southern Oscillation (ENSO), Pacific decadal variability, and Atlantic multidecadal variability. The solubility of CO_2 in the ocean is controlled both by water properties such as temperature and salinity and by biogeochemical tracers, e.g., dissolved inorganic carbon (DIC), transported by advection and diffusion. In addition, the air–sea CO_2 gas transfer velocity is a function of wind speed. Therefore, fluctuation of the physical properties related to the internal climate variations strongly perturbs the air–sea CO_2 flux (hereafter, CO2F, positive upward).
削除: strong
削除: CO2F
削除:). The strong
削除: during El Niño periods (warm sea surface temperature),
削除: waters and CO2F decrease
削除: reduced
削除: of cold DIC-rich deep water (
削除: fluctuations
削除: fluctuations
移動 (挿入) [1]
削除: Intergovernmental Panel on Climate Change (
削除:),
削除: sea surface temperature (
削除:)
削除: would be preferable
削除: employ an ESM capable of capturing this anticorrelated relationship between SST and CO2Funderstand

In this study, utilizing two kinds of ESMs to which observed ocean hydrographic data are assimilated, we attempted to identify the key processes to reproduce the observed historical air–sea CO_2 flux variations in the equatorial Pacific. The remainder of this paper is organized as follows. Sect. 2 provides a brief description of the models used in this study, and the derived results are presented in Sect. 3. Finally, a short discussion and a summary are presented in Sect. 4.

2 Methods

2.1 Model Description

In this study, we have conducted four experiments, NEW-assim, NEW, OLD-assim, and OLD. In NEW-assim and NEW, we used the MIROC-ES2L (Hajima et al., 2020) and in OLD-assim and OLD, we used the MIROC-ESM (Watanabe, S. et al., 2011). The former is newly developed for CMIP Phase 6 (CMIP6; Eyring et al., 2016), while the latter is an official model of CMIP5. The physical core model of MIROC-ES2L is MIROC5.2, which is a minor update of MIROC5 (Watanabe, M. et al. 2010; Tatebe et al. 2018), while that of MIROC-ESM is MIROC3m (K1 model developers, 2004). The horizontal resolution of the atmospheric component of MIROC-ES2L (MIROC-ESM) has T42 spectral truncation (i.e., approximately 300 km) with 40 (80) vertical levels up to 3 hPa (0.003 hPa). The oceanic component of MIROC-ES2L has a horizontal tripolar coordinate system. In the spherical coordinate portion south of 63°N, the longitudinal grid spacing is 1°, while the meridional grid spacing varies from approximately 0.5° near the equator to 1° in mid-latitude regions. There are 62 vertical levels in a hybrid σ–z coordinate system, the lowermost of which is located at the depth of 6300 m. The oceanic component of MIROC-ESM has a horizontal bipolar coordinate system: the longitudinal grid spacing of the oceanic component is approximately 1.4°, while the latitudinal grid intervals vary gradually from 0.5° at the equator to 1.7° near both poles. There are 44 vertical levels in a hybrid σ–z coordinate system, the lowermost of which is located at the depth of 5300 m. The resolutions in MIROC-ES2L are higher than in MIROC-ESM. In particular, 31 (21) of the 62 (44) vertical layers in MIROC-ES2L (MIROC-ESM) are within the upper 500 m of depth. The increased number of vertical layers in MIROC-ES2L has been adopted in order to better represent the equatorial thermocline.

In NEW-assim and OLD-assim, we used the ESMs that incorporated the same simple scheme for ocean data assimilation, which comprised an incremental analysis update (IAU; Bloom et al., 1996; Huang et al., 2002). This technique is relatively simple compared to more elaborate ones such as ensemble Kalman filter and four-dimensional variational method, but is widely used for decadal climate predictions (e.g., Mochizuki et al., 2010; Tatebe et al., 2012). Positive aspects of IAU is relatively low computational cost, which enables decadal-to-centennial scale integration and a variety of parameter sensitivity experiments. In the IAU, during the analysis interval from $t = 0$ to $t = \tau$, the governing equation including a correction term for temperature and salinity (X) is written as follows:

削除: For prediction of future physical states, previous studies used data assimilation systems to merge oceanic observational and/or reanalysis data for initialization of a physical climate model to the current phase of the internal climate variations. Variety of data assimilation techniques has been adopted, ranging from simple nudging technique (e.g., Behringer et al., 1998; Ji et al., 1998;In this

下へ移動 [2]: Smith et al., 2007; Keenlyside et al., 2008; Pohlmann et al., 2009; Sugiura et al., 2009;

下へ移動 [3]: Mochizuki et al., 2010; Tatebe et al., 2012

上へ移動 [1]: 2009; Tommasi et al., 2017a, 2017b; Park et al., 2018). Li et al. (2016, 2019) studied the predictability of CO2F

下へ移動 [4]: et al., 2011).

削除: Sugiura et al., 2009;

削除:) to more complex and computationally demanding techniques such as four-dimensional variational method or ensemble Kalman filter (e.g., Kalman, 1960; Sasaki, 1969, 1970; Evensen, 1994; Hunt et al., 2004; Kalnay et al., 2007; Yang et al., 2013). Furthermore, through incorporation into ESMs, the application of data assimilation systems has been expanded to include biogeochemical properties, e.g., CO2F monitoring, phytoplankton ... [1]

削除: Li et al. (2016, 2019) studied the predictability of CO2F ... [2]

削除: In this study, nudging technique is employed. The technique ... [3]

削除: used two ESMs, i.e., the MIROC-ESM, referred to hereafter ... [4]

削除: (Watanabe, S. et al., 2011)

削除: , referred to hereafter as NEW

移動 (挿入) [4]

削除:).

削除: an official model of CMIP5, while the latter is

削除:).

削除: OLD is MIROC3m, while that of NEW

削除: represents

削除: by

削除: (

削除: 2011).

書式を変更: フォント：ＭＳ 明朝

削除: OLD (NEW

削除: (40

削除: (3 hPa

削除: In OLD, the longitudinal grid spacing of the oceanic ... [5]

削除: 63

削除: this study, embedded in both

削除: was

移動 (挿入) [3]

削除: 2002).

$$\frac{dX}{dt} = \text{adv.} + \text{diff.} + F + \frac{\alpha}{\tau}\Delta X^a, \quad (1)$$

where adv. is the advection term, diff. is the diffusion term, F is the surface flux term, and the final term on the right-hand side is the correction term with α as a constant, and ΔX^a as the analysis increment. The analysis increment is calculated from $\Delta X^a = X^a(0) - X(0)$, where $X^a(0)$ is the analysis and $X(0)$ is the model first guess at $t = 0$; this term is held constant during the analysis interval. For $X^a(0)$ and $X(0)$, we used anomalies from monthly mean climatology during 1961–2000 in observations and models, respectively. Such a scheme often called 'anomaly assimilation' or 'anomaly initialization' is also used in many previous studies (e.g., Smith et al., 2007; Keenlyside et al., 2008; Pohlmann et al., 2009; Li et al., 2016, 2019; Sospedra-Alfonso and Boer, 2020). In addition, the IAU was applied at depths between the sea surface and 3000 m, with the values of $\tau = 1$ day and $\alpha = 0.025$ (Tatebe et al., 2012). The monthly objective analysis of ocean temperature and salinity (Ishii and Kimoto, 2009) are assimilated into the model as X^a, with linear interpolation to daily data. Because observed DIC concentration are sparse in space and time, only ocean hydrographic data are used for data assimilation in the present study. Also, any atmospheric observations/reanalysis are not applied.

Both of NEW and OLD are the exactly same as the historical simulations designated by CMIP6 and CMIP5 protocols, respectively, with three ensemble members for each which are bifurcated from arbitrary years of the corresponding preindustrial control simulations. The ocean data assimilation experiments, NEW-assim and OLD-assim, are bifurcated from NEW and OLD at the year 1946, respectively, and they are integrated up to the year 2005. Note that the data assimilation experiments are driven with the same external forcings as in the historical simulations. In the later sections, the model results in 1961–2005 are analyzed.

2.2 Estimating pCO_2 change at the sea surface

CO2F depends on the difference in CO_2 partial pressure between the sea and the air, i.e.:

$$\text{CO2F} = K(\text{pCO}_2 - \text{pCO}_2^{\text{air}})(1 - \gamma), \quad (2)$$

where pCO_2 (pCO_2^{air}) is the CO_2 partial pressure in the sea (air), γ is the fraction of sea ice, and $K = k\alpha$ is the CO_2 gas transfer coefficient, where k represents the CO_2 gas transfer velocity (Wanninkhof, 1992, 2014) and α represents the solubility of CO_2 in seawater (Weiss, 1974). The CO_2 gas transfer velocity k is a function of wind speed and the Schmidt number (Wanninkhof, 1992). This study investigated the reproducibility of the anticorrelated relationship between CO2F and SST and therefore the direction of the flux is important. As K does not affect the direction and the flux variation due to ENSO has larger amplitude in terms of pCO_2 than pCO_2^{air} (Dong et al., 2017), the direction of flux is governed by the variation in pCO_2. Consequently, we evaluated the pCO_2 change at the sea surface in the equatorial Pacific.

Seawater pCO_2 values depend on temperature (T), salinity (S), DIC concentration, and total alkalinity (Alk); therefore, the change of pCO_2 can be expanded as follows:

$$\Delta\text{pCO}_2 = C_{(T)} + C_{(S)} + C_{(DIC)} + C_{(Alk)} + \text{Res.}, \quad (3)$$

削除: Following Tatebe et al. (2012

移動 (挿入) [2]

削除: employed

削除: d

削除: .

削除: data

削除: were interpolated linearly to form daily analysis data, X^a. Hereafter, the OLD (NEW)are assimilated into the

削除: embedded with the IAU scheme is called OLD-assim (NEW-assim).as

削除: OLD and NEW were integrated for spinup under preindustrial forcing until reaching an equilibrium state. Then, a set of historical runs with external forcing based on observations from 1850 through to 2005 (i.e., the end year of the historical run in CMIP5) was conducted. Note that OLD and OLD-assim (NEW and NEW-assim) were driven with CMIP5 (CMIP6) forcing. Data assimilation started at 1946 to reflect the time span of observed ocean data. The model results from 1961–2005 were used for analysis. There were three ensemble members for each run of OLD/NEW and OLD/NEW-assim.Both of

書式を変更: 下付き

削除: $\frac{\partial \text{pCO}_2}{\partial \text{T}}\Delta\text{T} + \frac{\partial \text{pCO}_2}{\partial \text{S}}\Delta\text{S} + \frac{\partial \text{pCO}_2}{\partial \text{DIC}}\Delta\text{DIC} + \frac{\partial \text{pCO}_2}{\partial \text{Alk}}\Delta\text{Alk} +$

where C(X) = ($\partial pCO_2/\partial X$)ΔX (X=T, S, DIC, Alk) is the pCO_2 change due to the change in X (X=T, S, DIC, Alk), and Res., which includes second-order terms (Takahashi et al., 1993), was estimated so that the left-hand side and right-hand sides in Eq. (3) are equal in this study. In Sect. 3, we evaluate the CO2F and pCO_2 variations in the equatorial Pacific in NEW-assim, NEW, OLD-assim, and OLD, and we calculate each term in Eq. (3) for each experiment.

削除: as $\Delta pCO_2 - (\partial pCO_2/\partial T)\Delta T - (\partial pCO_2/\partial S)\Delta S - (\partial pCO_2/\partial DIC)\Delta DIC - (\partial pCO_2/\partial Alk)\Delta Alk$…
削除: first
削除: fluctuations
削除: both
削除: and
削除: model

2.3 Observation and reanalysis dataset

To assess CO2F, ocean temperature, and wind speed of the model output, we used observation or reanalysis datasets. As the CO2F dataset, we used the SOM-FFN (Landschützer et al., 2016, 2018). It is an estimate based on the ocean surface CO_2 observation data collection, SOCATv3 (Bakker et al., 2016), and provides monthly data since 1982. It shows significant interannual variation of CO2F in some specific regions such as the equatorial Pacific and high latitudes of both hemispheres (Figure S1). In Sect. 3, we focus on the CO2F in the Niño3 region (5°S–5°N, 150°W–90°W) which shows notable variation of CO2F in the equatorial Pacific. This region is also the maximum variability region for SST (Gill, 1980). As the SST dataset, the observational COBE-SST2 (Ishii et al., 2005; Hirahara et al., 2014) was used. The JRA55 reanalysis (Kobayashi et al., 2015) was used for wind speed dataset.

移動 (挿入) [5]
移動 (挿入) [6]

3 Results

3.1 CO_2 flux and pCO_2 anomalies in Niño3 region

書式を変更: 下付き
書式を変更: 下付き
削除: anomaly
削除: time

Horizontal maps for correlation coefficients between simulated and observed CO2F are shown in Figure 1. The model output data were ensemble mean and linearly interpolated into the SOM-FFN grid. Note that the data were not detrended, and one-year running mean filter is applied to monthly COF2 anomalies in 1982–2005 before calculating the correlation coefficients in accordance with the period for which the SOM-FFN dataset is available. CO2F in NEW-assim shows a positive correlation with SOM-FFN in the equatorial Pacific region (Figure 1a) where significant interannual variations of CO2F are found (Figure S1). On the other hand, CO2F in OLD-assim (Figure 1c) is negatively correlated in the equatorial Pacific. The timeseries in the Niño3 region of both one-year running mean SST (hereafter, NINO3-SST) and CO2F (hereafter, NINO3-CO2F) anomalies simulated with NEW-assim (OLD-assim) are shown in Figure 1b (Figure 1d). Here, the data were detrended and monthly anomalies were calculated with respect to the 1971–2000 monthly mean climatology. The correlation coefficients between NINO3-SST and NINO3-CO2F anomalies in NEW-assim, OLD-assim, and observation are –0.50, 0.44, and –0.75, respectively (Table 1). The results in NEW-assim are consistent with the observations, while those in OLD-assim are not. The correlation coefficients between NINO3-SST and NINO3-CO2F anomalies in NEW and OLD are –0.85 and –0.67, respectively (Table 1 and Figure S2). Note that OLD could capture the

削除: (5°S–5°N, 90°–150°W)
削除: (NEW-assim
削除: Figure 1a (
削除:). The correlation coefficient
削除: in NEW-assim (OLD-assim) is –0.41 (0.44). It suggests that the observed anticorrelated relationship is captured well in NEW-assim but not in…
削除: . Dong et al. (2016) showed

observed anticorrelated relationship between NINO3-SST and NINO3-CO2F anomalies, but OLD-assim could not reproduce this relationship.

As the vertical direction of CO2F is determined mainly by pCO_2 at the sea surface (see Eq. (2)), we further estimated each term in Eq. (3) for each model output (Figure 2). In order to evaluate C(X) in Eq. (2) (X = pCO_2, T, S, DIC, or Alk), we estimated ΔX by averaging monthly mean X anomalies regressed on the NINO3-SST anomalies over the entire Niño3 region, while $\partial pCO_2/\partial X$ was estimated based on the climatological annual mean T, S, DIC, and Alk at the sea surface within the Niño3 region in each experiment. In the following, we describe the anomalies during El Niño periods, while the opposite applies during La Niña periods. In NEW-assim, NEW, and OLD, pCO_2 decreases because the effect of the decrease in pCO_2 with decreasing DIC concentrations is larger than that of the increase in pCO_2 with warming (Figure 2). In OLD-assim, however, the effect of the increase in pCO_2 with warming is larger than that of OLD, and the decrease in pCO_2 with decreasing DIC concentrations is smaller than that of OLD, resulting in an increase in pCO_2. As noted in Sect. 1, previous studies (Le Borgne et al., 2002; Feely et al., 2004; Doney et al., 2009a, 2009b) showed that variability in upwelling during ENSO events dominates the equatorial Pacific CO2F variations through its regulation of DIC. In the following, we discuss the temperature and vertical velocity changes associated with ENSO along the Equator.

3.2 DIC and vertical velocity changes

A cross section of the monthly ocean temperature anomalies regressed onto monthly mean NINO3-SST anomalies along the equatorial Pacific is presented in Figure 3, together with the climatological annual mean depths of the 18, 20, and 22 °C isotherms. Here, monthly temperature anomalies were calculated with respect to the 1971–2000 monthly mean climatology. The observational temperature anomalies as well as the climatological isotherms are derived from the monthly objective analysis of ocean temperature (Ishii and Kimoto, 2009). Amplitudes of the positive (negative) equatorial temperature anomalies in the upper (lower) layer of the eastern (western) equatorial Pacific in NEW are larger than in OLD and are closer to observations. The intensity of ENSO defined as the standard deviation of detrended one-year running mean NINO3-SST anomalies from 1961 to 2005 is shown in Table 2. The intensity of ENSO in NEW is estimated to be 1.17 °C (Table 2), a bit stronger than the observation (0.80 °C). On the other hand, the intensity of ENSO in OLD is 0.43 °C, which is about a half as large as that in observations. In addition, the climatological mean thermocline in NEW is tighter than in OLD and is closer to observations. The improvement in ENSO reproducibility in NEW is attributable mainly to two updates in the model configuration. The first is implementation of an updated plume model for cumulus convection with multiple cloud types where lateral entrainment rate varies vertically depending on the surrounding environment (Chikira and Sugiyama, 2010). The state-dependent lateral entrainment affects the strength of convectively-induced air–sea coupled processes in the eastern tropical Pacific, and thus the ENSO amplitude in the model. More details are described in Watanabe et al. (2010). The second is reduction of numerical diffusion by introducing highly-accurate tracer advection scheme in the ocean and by increasing vertical resolutions (Prather, 1986). The equatorial thermocline in the climatic-mean state of the

削除: in the equatorial Pacific; however,
削除: We estimated ΔX
削除:) in Eq. (3) as X
削除: averaged
削除: model
削除: impact
削除: change
削除: concentration (i.e., the absolute value of ($\partial pCO_2/\partial DIC$)ΔDIC)
削除: change in CO_2 solubility due to temperature
削除: (i.e., ($\partial pCO_2/\partial T$)ΔT) and thus Δ$pCO_2$ becomes negative during El Niño periods. However,in pCO
削除: ($\partial pCO_2/\partial T$)ΔT
削除: in
削除: absolute value of (∂
削除: /∂
削除:)ΔDIC
削除: positive ΔpCO_2 during El Niño periods. In NEW and NEW-assim, the absolute value of ($\partial pCO_2/\partial DIC$)ΔDIC is large, causing negative ΔpCO_2.…
削除: upwelling
削除: during El Niño periods
削除: **upwelling**
削除: **in OLD and OLD-assim**
削除: Here, we analyze the model results of both OLD-assim and OLD. A cross section of the monthly ocean temperature anomaly
削除: anomaly
削除: Equator within the
削除: In comparison with observations (Figure 3c) (Ishii and Kimoto, 2009), the climatological mean state of OLD shows an equatorial thermocline that is more diffuse than observed. In addition, the The observational
削除: increase during El Niño periods in OLD is smaller (Figure 3a). The standard deviation of NINO3-SST in OLD was
削除: 0.43 °C, i.e., approximately half that
削除: COBESST2 dataset (0.71 °C)
上へ移動 [6]: (Ishii et al., 2005; Hirahara et al., 2014
削除:). Our result is consistent with Meehl et al. (2001), who ... [6]
削除: difference between the top and bottom of the thermocline is ... [7]
削除: central
削除: as the zonal wind anomaly at 10 m height above the sea ... [8]
削除: regression of NINO4-U10 over NINO3-SST (m s^{-1} $°C^{-1}$) ... [9]
削除: OLD. The wind (vertical velocity) feedback of 0.46 m s^{-1} °C ... [10]
削除: half that evaluated

tropical Pacific is more diffuse in OLD than in observation, which is partly arisen from numerical diffusion, especially in vertical advection (Tatebe and Hasumi, 2010), and this model bias is much alleviated in NEW. Correspondingly, so-called thermocline mode (e.g., Imada et al., 2006) becomes more effective and ENSO amplitude becomes larger in NEW. As the ENSO amplitude in NEW is larger than in OLD, the variation of the equatorial trade wind, which causes anomalous equatorial vertical velocity, is also larger in NEW.

To assess the variations of zonal wind associated with ENSO, we estimated the 10 m zonal wind anomalies over the NINO4 region (5°S–5°N, 160°E–150°W; the dotted line boxes in Figure 1a) which are regressed onto the NINO3-SST anomalies (Table 3). Niño4 region is the maximum variability region for the equatorial trade wind (Figure S3). Hereafter, the above-mentioned regression coefficient is referred to as wind feedback. The positive value of wind feedback in NEW (0.92 m s^{-1} K^{-1}) indicates an westerly wind anomalies during El Niño, and this is consistent with that evaluated from the observational dataset, i.e., 1.02 m s^{-1} K^{-1}. The wind feedback in OLD (0.46 m s^{-1} K^{-1}) is about half of NEW and the observation.

Cross sections of the monthly upward water velocity and DIC concentration anomalies along the equator regressed onto NINO3-SST anomalies in NEW (OLD) are shown in Figure 4a and 4c (Figure 4b and 4d), respectively. By reproducing wind feedback that is consistent with the observation, the westerly wind anomalies during El Niño periods in NEW (Figure S3c) is comparable to that of the JRA55 reanalysis (Figure S3i), leading to weakening of upward vertical velocity of approximately 5 × 10^{-6} m s^{-1} (Figure 4a). This weakening of upward vertical velocity causes decrease in surface DIC in the eastern equatorial Pacific during El Niño periods (Figure 4c). In OLD, the smaller wind feedback and associated smaller westerly wind anomalies than in the JRA55 reanalysis (Figure S3g) leads to weakening of upward vertical velocity of just 10^{-6} m s^{-1} in the equatorial Pacific (Figure 4b). Although the ENSO signal in OLD is weaker than the observation, because of decrease in upward vertical velocity from normal years, the surface DIC concentration decreases during El Niño periods (Figure 4d). This is consistent with Dong et al. (2016), showing that OLD is able to qualitatively reproduce the negative correlation between SST and DIC concentration anomalies in the eastern equatorial Pacific (Figure S2b).

Next, we examined the correction term in temperature due to the data assimilation, i.e., temperature analysis increment, the final term on the right-hand side of Eq. (1), and the variations in vertical velocity and DIC concentration. Anomalies of monthly mean temperature analysis increments, vertical velocity, and DIC concentration along the equator regressed onto NINO3-SST anomalies are shown in Figure 5. The maximum absolute value of the equatorial temperature analysis increment in NEW-assim is found at 10–40 m depths in the eastern equatorial Pacific, shallower than the depth of the thermocline (Figure 5a). In NEW-assim, the wind feedback is 0.92 m s^{-1} K^{-1} (Table 3), which is of the same magnitude to that in NEW (0.92 m s^{-1} K^{-1}), and the surface wind anomalies still shows similar pattern to that of the NEW (Figure S3a–d). The westerly wind anomalies in NEW-assim leads to weakening of upward vertical velocity along the equator during El Niño periods (Figure 5c). To assess the variation in equatorial vertical velocity associated with ENSO, we estimated the anomalies of the vertical velocity at the depth of the 20 °C isotherm (the depth of the thermocline) in the Niño3 region which are regressed onto the NINO3-SST anomalies. Hereafter, the regression coefficient is referred to as vertical velocity

削除: the JRA55 reanalysis wind dataset (Kobayashi et al., 2015)

削除: the COBESST2 dataset (Ishii et al., 2005; Hirahara et al., 2014), i.e., 1.02 m s^{-1} $°C^{-1}$ (thin dashed line in Figure 4)….

削除: in OLD without assimilation are shown in Figure 5a and 5b, respectively. The weak ENSO signal in the zonal wind in OLD (Figure 4) leads to a decrease in water upwelling of just 10^{-6} m s^{-1} in the equatorial Pacific (Figure 5a). Although the ENSO signal in OLD (without assimilation) is weak because of weakened upwelling of subsurface DIC-rich waters (Figure 5a), the DIC concentration of the surface waters decreases (Figure 5b). This is consistent with Dong et al. (2016), showing that OLD is able to reproduce qualitatively the anticorrelated relationship between temperature and DIC concentration.
We investigated the correction in temperature due to the data assimilation (temperature increment, the final term on the right-hand side of Eq. (1)) and the fluctuations in vertical velocity and DIC concentration in OLD-assim. The monthly mean temperature increment, vertical velocity, and DIC concentration along the Equator regressed onto NINO3-SST …

削除: 6a–c, respectively. As the temperature increase during El Niño periods in OLD is smaller than observed (Figure 3a and 3c), data assimilation causes the water temperature to increase by 0.16 × 10^{-6} °C s^{-1} at the depth of the thermocline (the depth of the 20 °C isotherm) in the eastern equatorial Pacific (Figure 6a). The 4

削除: in OLD-assim is 0.49 m s^{-1} $°C^{-1}$ (red cross in Figure 4), which is the same as in OLD; however, the strong heating causes upwelling of DIC-rich waters in the subsurface layers (Figure 6b). The positive value of vertical velocity feedback in Figure 4 indicates enhancement of subsurface cold water upwelling and weakening of the SST increase. This unrealistically prevents El Niño from developing fully. This upwelling also causes the DIC concentration ... [11]

上へ移動 [5]: In Sect.

削除: 3.2, El Niño is associated with both a

削除: anomaly in the central equatorial Pacific and a vertical velocity anomaly in the eastern equatorial Pacific. The wind ... [12]

削除: much larger than in OLD (0.46 m s^{-1} $°C^{-1}$). We also note that this is comparable with

削除: with

削除: evaluated from

削除: Kobayashi et al., 2015), i.e., 1.02 m s^{-1} $°C^{-1}$. Thus, based on the fluctuations in water temperature and wind speed, it can be said ... [13]

削除: anomaly regressed onto NINO3-SST in NEW is shown in Figure 7a. The stronger ENSO signal in the zonal wind in NEW in ... [14]

削除: . The

削除: feedback is estimated as −0.47 × 10^{-6} m s^{-1} $°C^{-1}$ (black circle

削除: Figure 4). A cross section of the monthly

削除: concentration anomaly regressed onto NINO3-SST is shown

削除: 7b. Owing to

削除: anomaly and the decrease in upwelling, NEW is able to reproduce the realistic decrease in DIC concentration during El Niño ... [15]

削除: Here, we investigate the model results of NEW-assim. The monthly temperature increment, vertical velocity, and DIC ... [16]

feedback. The vertical velocity feedback in NEW-assim is estimated to be -4.5×10^{-7} m s^{-1} K^{-1}, which is not significantly different from that in NEW (-3.9×10^{-7} m s^{-1} K^{-1}) (Table 3). The negative value of vertical velocity feedback in NEW-assim indicates the weakening of upward vertical velocity at the depth of the thermocline during El Niño periods in the eastern equatorial Pacific (Figure 5c). The weakening of upward vertical velocity causes lesser supply of the DIC-rich subsurface water to the surface layer, leading to the decrease in surface DIC concentration (Figure 5e). In OLD, the temperature variations associated with ENSO at the depth of the thermocline in the eastern equatorial Pacific is smaller than observed (see Figure 3b and 3c), so that the correction term forces to raise the equatorial water temperature by 0.16×10^{-6} °C s^{-1} during El Niño periods in order to realize observed temperature variations (Figure 5b). The wind feedback in OLD-assim is 0.48 m s^{-1} K^{-1} (Table 3), which is the same as in OLD, and the map of the wind speed anomalies shows a similar pattern to that of the OLD (Figure S3e–h); however, the warming due to data assimilation procedure during El Niño periods reduces density, leading to low-pressure anomalies. This results in anomalous cyclonic circulation and convergence, and thus enhancement of upward vertical velocity at the depth of the thermocline (Figure 5d). The vertical velocity feedback in OLD-assim is 4.1×10^{-7} m s^{-1} K^{-1}, which has an opposite sign to OLD, -4.9×10^{-7} m s^{-1} K^{-1} (Table 3). The positive value of vertical velocity feedback indicates the enhancement of upward vertical velocity at the depth of the thermocline during El Niño periods, which is inconsistent with observations. This spurious enhancement of upward vertical velocity during El Niño periods causes the increase in the surface DIC concentration (Figure 5f), leading to positive correlation between SST and CO2F (Figure 1d), contrary to observations. We have to note here that even in the NEW-assim, the vertical velocity distribution (Figure 5c) is still different from NEW (Figure 4a) because of the temperature analysis increment. As already discussed, the intensity of ENSO in NEW is slightly stronger than observed (Table 2). In addition, the period of ENSO, which is defined as the peak of the power spectrum of one-year running mean NINO-SST, is 5.0 years in NEW, which is longer than 3.5 years of observations (see Table 2). Because the ENSO characteristics in NEW are not perfectly consistent with observations, model nature, namely responses of vertical velocity and DIC concentration in ENSO, are still distorted by the temperature analysis increment even in NEW-assim. This indicates that further model improvements are needed.

4 Discussion and Summary

In the present study, comparing the results of two ESMs to which observed ocean hydrographic data are assimilated, we have clarified that representation of the processes in the equatorial climate system is important to reproduce the observed anticorrelated relationship between SST and CO2F in the equatorial Pacific. In the case where the ocean temperature and salinity observations were assimilated into an ESM with weaker amplitude of ENSO than observations, the correction term on the governing equation of the ocean temperature, which was introduced in the data assimilation procedure, caused spurious upwelling (downwelling) anomalies along the equator during El Niño (La Niña) periods, leading to more (less) supply of the DIC-rich subsurface water to the surface layer. Due to the resultant increase (decrease) of the surface

削除: The equatorial Pacific is

削除: region where most prominent interannual variability of CO2F can be seen (e.g., Park et al., 2010; Valsala and Maksyutov, 2010; Landschützer et al., 2014; Rödenbeck et al., 2014). In this

削除: same simple data assimilation scheme is incorporated into

削除: , OLD in

削除: the ENSO amplitude is about half the

削除: value and NEW with improved reproducibility of ENSO. The correlationocean hydrographic data are assimilated,

削除: is consistently represented only

削除: are

削除: NEW. Response of the equatorial trade wind to the observed SST was significantlyan ESM with

削除: observed in OLD with the data assimilation, which cannot support the development of the equatorial subsurface temperature variations during El Niño periods with comparable amplitude in

削除: . Instead, relative importance of

削除: is

削除: becomes nonnegligible, and advection-diffusion balance of the temperature is biased with respect to model's physical nature. Resultantcaused

削除: equatorial

削除: of

削除: DIC-rich

削除: works

DIC concentration, the upward (downward) CO2F anomalies during El Niño (La Niña) periods was induced, which was inconsistent with observation. In the case where the ocean temperature and salinity observations were assimilated into the other ESM with rather realistic ENSO representation, anticorrelated relationship between SST and CO2F was reproduced.

Focusing on the CO2F fluctuations associated with ENSO in the equatorial Pacific, Dong et al. (2016) analyzed the results of the CMIP5 ESMs. They showed that only a portion of CMIP5 ESMs (including MIROC-ESM) could reproduce the observed anticorrelated relationship between SST and CO2F. Bellenger et al. (2014) evaluated the reproducibility of ENSO in the CMIP5 models. They reported that most CMIP5 climate models and ESMs underestimate the amplitude of the wind stress feedback by 20%–50%, and that only 20% of CMIP5 models have relative error within 25% of the observed value. There are many ESMs where the ENSO characteristics and/or the SST-CO2F relationship are inconsistent with observations. Causes of this discrepancy should be addresses in future studies through, for example, multi-model analysis, and also process-based uncertainty estimation will be further required in initialized climate and carbon predictions as well as projections by ESMs.

削除: periods, and thus, unrealistic upward

削除: occurs in the case where the data assimilation is incorporated into OLD. We conclude that faithful representation of the processes in the equatorial climate system is crucial for improved initialization and subsequent prediction in marine ecosystem modeling.was

削除: OLD

削除: Our study indicated that reliable future prediction of CO2F in the equatorial Pacific would benefit from faithful reproduction of wind feedback in ESMs that is sufficiently strong to capture the anticorrelated relationship between SST and CO2F, even with data assimilationThere are many ESMs where the ENSO

削除: In this study, as a first step toward predicting fluctuations in atmospheric CO_2 concentration, we discussed fluctuations in CO2F attributable directly to ENSO. It is also known that CO2F fluctuates in association with Pacific decadal variability (Valsala et al., 2012) and Atlantic multidecadal variability (Breeden and McKinley, 2016). In addition, land–air CO_2 flux also fluctuates in association with ENSO (Eldering et al., 2017). The reproducibility of fluctuations in CO2F in other regions as well as those of land–air CO_2 flux remains a topic for future research.

Data availability

The model outputs of MIROC-ES2L (Hajima et al., 2019) are available through the Earth System Grid Federation (ESGF) (https://doi.org/10.22033/ESGF/CMIP6.5602). The model outputs of MIROC-ESM is also available at ESGF, https://esgf-node.llnl.gov/projects/cmip5/. The CMIP6 forcing data is version 6.2.1, and the CMIP5 forcing data is described at https://pcmdi.llnl.gov/mips/cmip5/forcing.html. The JRA55 reanalysis wind dataset is available at https://jra.kishou.go.jp/JRA-55/index_en.html. The COBE-SST2 dataset is available at https://www.esrl.noaa.gov/psd/data/gridded/data.cobe2.html. The postprocessing scripts used for this research and the data used in the figures can be obtained online (https://osf.io/mpk52).

削除: and the CMIP6 forcing data is version 6.2.1

削除: COBESST2

Author contribution

MiW, HT, MaW, and MK contributed to the experiment design. MiW and HK embedded the ocean data assimilation system into the ESMs. MiW and TH performed the experimental simulations. MiW analyzed the model output and drafted the paper. All authors discussed the results, and commented on and edited the manuscript.

Competing interests

The authors declare that they have no conflict of interest.

Acknowledgments

This work was supported by the Integrated Research Program for Advanced Climate Models (TOUGOU) Grant Numbers JPMXD0717935457 and JPMXD0717935715 from the Ministry of Education, Culture, Sports, Science and Technology, MEXT, Japan. We thank B. Barton, J. Jardine, M. Payo Payo, C, Unsworth and one anonymous reader for helpful comments. We also thank three anonymous reviewers provided many helpful suggestions for improving the article.

References

Bakker, D. C. E., et al.: A multi-decade record of high-quality fCO_2 data in version 3 of the Surface Ocean CO_2 ATlas (SOCAT), Earth Syst. Sci. Data, 8, 383–413, doi:10.5194/essd-8-383-2016, 2016.

Behringer, D. W., Ji, M., and Leetmaa, A.: An improved coupled model for ENSO prediction and implications for ocean initialization. Part I: The ocean data assimilation system, Mon. Weather Rev., 126, 1013–1021, doi:10.1175/1520-0493(1998)126<1013:AICMFE>2.0.CO;2, 1998

Bellenger, H., Guilyardi, E., Leloup, J., Lengaigne, M., and Vialard, J.: ENSO representation in climate models: From CMIP3 to CMIP5, Clim. Dyn., 42, 1999–2018, doi:10.1007/s00382-013-1783-z, 2014.

Bloom, S. C., Takacs, L. L., da Silva, A. M., and Ledvina, D.: Data assimilation using incremental analysis updates, Mon. Weather Rev., 124, 1256–1271, 1996.

Brasseur, P., Gruber, N., Barciela, R., Brander, K., Doron, M., El Moussaoui, A., Hobday, A. J., Huret, M., Kremeur, A.-S., Lehodey, P., Matear, R., Moulin, C., Murtugudde, R., Senina, I., and Svendsen, E.: Integrating biogeochemistry and ecology into ocean data assimilation systems, Oceanography, 22(3), 206–215, doi:10.5670/oceanog.2009.80, 2009.

Chikira, M., and Sugiyama, M.: A cumulus parameterization with state-dependent entrainment rate. Part I: Description and sensitivity to temperature and humidity profiles, J. Atmos. Sci., 67, 2171–2193, doi:10.1175/2010JAS3316.1, 2010.

Doney, S. C., Bopp, L., and Long, M. C.: Historical and future trends in ocean climate and biogeochemistry, Oceanography, 27(1), 108–119, doi:10.5670/oceanog.2014.14, 2014.

Doney, S. C., Balch, W. M., Fabry, V. J., and Feely, R. A.: Ocean acidification: A critical emerging problem for the ocean sciences, Oceanography, 22(4), 16–25, doi:10.5670/oceanog.2009.93, 2009a.

削除: Breeden, M. L., and McKinley, G. A.: Climate impacts on multidecadal pCO_2 variability in the North Atlantic: 1948–2009, Biogeosciences, 13, 3387–3396, doi:10.5194/bg-13-3387-2016, 2016.

Doney, S. C., Fabry, V. J., Feely, R. A., and Kleypas, J. A.: Ocean acidification: The other CO_2 problem, Annu. Rev. Mar. Sci., 1, 169–192, doi:10.1146/annurev.marine.010908.163834, 2009b.

Dong, F., Li, Y., Wang, B., Huang, W., Shi, Y., and Dong, W.: Global air–sea CO_2 flux in 22 CMIP5 models: Multiyear mean and interannual variability, J. Clim., 29, 2407–2431, doi:10.1175/JCLI-D-14-00788.1, 2016.

Dong, F., Li, Y., and Wang, B.: Assessment of responses of Tropical Pacific air–sea CO_2 flux to ENSO in 14 CMIP5 models, J. Clim., 30, 8595–8613, doi:10.1175/JCLI-D-16-0543.1, 2017.

Evensen, G.: Sequential data assimilation with a nonlinear quasi-geostrophic model using Monte Carlo methods to forcast error statistics, J. Geophys. Res., 99, 10143–10162. 1994.

Eyring, V., Bony, S., Meehl, G. A., Senior, C. A., Stevens, B., Stouffer, R. J., and Taylor, K. E.: Overview of the Coupled Model Intercomparison Project Phase 6 (CMIP6) experimental design and organization, Geosci. Model Dev., 9, 1937–1958, doi:10.5194/gmd-9-1937-2016, 2016.

Feely, R. A., Wanninkhof, R., Goyet, C., Archer, D. E., and Takahashi, T.: Variability of CO_2 distributions and sea–air fluxes in the central and eastern equatorial Pacific during the 1991–1994 El Niño, Deep-Sea Res. II, 44, 1851–1867, doi:10.1016/S0967-0645(97)00061-1, 1997.

Feely, R. A., Wanninkhof, R., Takahashi, T., and Tans, P.: Influence of El Niño on the equatorial Pacific contribution to atmospheric CO_2 accumulation, Nature, 398, 597–601, doi:10.1038/19273, 1999.

Feely, R. A., Wanninkhof, R., McGillis, W., Carr, M.-E., and Cosca, C. E.: Effects of wind speed and gas exchange parameterizations on the air–sea CO_2 fluxes in the equatorial Pacific Ocean, J. Geophys. Res., 109, C08S03, doi:10.1029/2003JC001896, 2004.

Gill., A. E.: Some simple solutions for heat-induced tropical circulation, Quart. J. Roy. Meteor. Soc., 106, 447–462, 1980.

Guilyardi, E, Braconnot, P., Jin, F.-F., Kim, S. T., Kolasinski, M., Li, T., and Musat, I.: Atmosphere feedbacks during ENSO in a coupled GCM with a modified atmospheric convection scheme, J. Clim., 22, 5698–5718, doi:10.1175/2009JCLI2815.1, 2009.

Hajima, T., Abe, M., Arakawa, O., Suzuki, T., Komuro, Y., Ogura, T., Ogochi, K., Watanabe, M., Yamamoto, A., Tatebe, H., Noguchi, M. A., Ohgaito, R., Ito, A., Yamazaki, D., Ito, A., Takata, K., Watanabe, S., Kawamiya, M., and Tachiiri, K.: MIROC MIROC-ES2L model output prepared for CMIP6 CMIP historical, Earth System Grid Federation, available at: https://doi.org/10.22033/ESGF/CMIP6.5602, 2019.

Hajima, T., Watanabe, M., Yamamoto, A., Tatebe, H., Noguchi, M. A., Abe, M., Ohgaito, R., Ito, A., Yamazaki, D., Okajima, H., Ito, A., Takata, K., Ogochi, K., Watanabe, S., and Kawamiya, M.: Description of the MIROC-ES2L Earth system model and evaluation of its climate–biogeochemical processes and feedback, Geosci. Model Dev., doi:10.5194/gmd-2019-275, accepted, 2020.

Hirahara, S., Ishii, M., and Fukuda, Y.: Centennial-scale sea surface temperature analysis and its uncertainty, J. Clim., 27, 55–75, doi:10.1175/JCLI-D-12-00837.1, 2014.

削除: Eldering,

下へ移動 [7]: A.,

削除: Wennberg, P. O., Crisp, D., Schimel, D. S., Gunson, M. R., Chatterjee, A., Liu, J., Schwandner, F. M., Sun, Y., O'Dell, C. W., Frankenberg, C., Taylor, T., Fisher, B., Osterman, G. B., Wunch, D., Hakkarainen, J., Tamminen, J., and Weir, B.: The Orbiting Carbon Observatory-2 early science investigations of regional carbon dioxide fluxes, Science, 358, eaam5745, doi:10.1126/science.aam5745, 2017.

移動 (挿入) [7]

Huang, B., Kinter, J. L., and Schopf, P. S.: Ocean data assimilation using intermittent analyses and continuous model error correction, Adv. Atmos. Sci., 19, 965–992, doi:10.1007/s00376-002-0059-z, 2002.

Imada, Y., and Kimoto, M.: Improvement of thermocline structure that affect ENSO performance in a coupled GCM, SOLA 2, 164–167, doi:10.2151/sola.2006–042, 2006.

Intergovernmental Panel on Climate Change (IPCC): Climate change 2013: The physical science basis, in Contribution of Working Group I to the Fifth Assessment Report of the Intergovernmental Panel on Climate Change, edited by Stocker, T. F., Qin, D., Plattner, G.-K., Tignor, M., Allen, S. K., Boschung, J., Nauels, A., Xia, Y., Bex, V., and Mdgley, P. M., p. 1535, Cambridge University Press, Cambridge, U.K.; New York, NY, USA, 2013.

Intergovernmental Panel on Climate Change (IPCC): Global warming of 1.5°C. An IPCC Special Report on the impacts of global warming of 1.5°C above pre-industrial levels and related global greenhouse gas emission pathways, in the context of strengthening the global response to the threat of climate change, sustainable development, and efforts to eradicate poverty, edited by Masson-Delmotte, V., et al., Cambridge University Press, Cambridge, U.K., 2018

Ishii, M., and Kimoto, M.: Reevaluation of historical ocean heat content variations with time-varying XBT and MBT depth bias corrections, J. Oceanogr., 65, 287–299, doi:10.1007/s10872-009-0027-7, 2009.

Ishii, M., Shouji A., Sugimoto, S., and Matsumoto, T.: Objective analyses of sea-surface temperature and marine meteorological variables for the 20th century using ICOADS and the Kobe Collection, Int. J. Climatol., 25, 865–879, doi:10.1002/joc.1169, 2005.

Ji, M., Behringer, D. W., and Leetmaa, A.: An improved coupled model for ENSO prediction and implications for ocean initialization. Part II: The coupled model, Mon. Weather Rev., 126, 1022–1034, doi:10.1175/1520-0493(1998)126<1022:AICMFE>2.0.CO;2, 1998.

Jones, C. D., Collins, M., Cox, P. M., and Spall, S. A.: The carbon cycle response to ENSO: A coupled climate–carbon cycle model study, J. Clim., 14, 4113–4129, doi:10.1175/1520-0442(2001)014<4113:TCCRTE>2.0.CO;2, 2001.

K-1 model developers: K-1 coupled GCM (MIROC) description, K-1 Tech. Rep., 1, edited by: Hasumi, H. and Emori, S., Center for Climate System Research, the Univ. of Tokyo, Tokyo, 34 pp., 2004.

Kalman, R. E.: A new approach to linear filtering and prediction problems, Trans. ASME J. Basic Eng., 82, 35–45, 1960.

Kalnay, E., Li, H., Miyoshi, T., Yang, S.-C., and Ballabrera-Poy, J.: 4-D-Var or ensemble Kalman filter?, Tellus, 59A, 758–773. doi:10.1111/j.1600-0870.2007.00261.x, 2007.

Kawamiya, M., Hajima, T., Tachiiri, K., and Yokohata, T.: Two decades of Earth system modeling, submitted to Prog. Earth Planetary Sci., 2019.

Keeling, C. D., and Revelle, R.: Effects of El Niño/Southern Oscillation on the atmospheric content of carbon dioxide, Meteoritics, 20, 437–450, 1985.

Keenlyside, N. S., Latif, M., Jungclaus, J., Kornblueh, L., and Roeckner, E.: Advancing decadal-scale climate prediction in the North Atlantic sector, Nature, 453, 84–88, doi:10.1038/nature06921, 2008.

Kobayashi, S., Ota, Y., Harada, Y., Ebita, A., Moriya, M., Onoda, H., Onogi, K., Kamahori, H., Kobayashi, C., Endo, H., Miyaoka, K., and Takahashi, K.: The JRA-55 Reanalysis: General specifications and basic characteristics, J. Meteorol. Soc. Japan, 93(1), 5–48, doi:10.2151/jmsj.2015-001, 2015.

Locarnini, R. A., Mishonov, A. V., Antonov, J. I., Boyer, T. P., Garcia, H. E., Baranova, O. K., Zweng, M. M., Paver, C. R., Reagan, J. R., Johnson, D. R., Hamilton, M., and Seidov, D.: World Ocean Atlas 2013, Volume 1: Temperature. Levitus, S., Ed., Mishonov, A., Technical Ed.; NOAA Atlas NESDIS 73, 40 pp., 2013.

Landschützer, P., Gruber, N., Bakker, D. C. E., and Schuster, U.: Recent variability of the global ocean carbon sink, Glob. Biogeochem. Cycles, 28, 927–949, doi:10.1002/2014GB004853, 2014.

Landschützer, P., Gruber, N., and Bakker, D. C. E.: Decadal variations and trends of the global ocean carbon sink. Global Biogeochem. Cycles 30, 1396–1417, doi: 10.1002/2015GB005359, 2016.

Landschützer, P., Gruber, N., Bakker, D. C. E., Stemmler, I., and Six, K. D.: Strengthening seasonal marine CO_2 variations due to increasing atmospheric CO2. Nat. Clim. Change 8, 146–150, doi: 10.1038/s41558-017-0057-x, 2018.

Le Borgne, R., Feely, R. A., and Mackey, D. J.: Carbon fluxes in the equatorial Pacific: A synthesis of the JGOFS programme, Deep-Sea Res. II, 49, 2425–2442, doi:10.1016/S0967-0645(02)00043-7, 2002.

Lengaigne, M., Hausmann, U., Madec, G., Menkes, C., Vialard, J., and Molines, J. M.: Mechanisms controlling warm water volume interannual variations in the equatorial Pacific: Diabatic versus adiabatic processes, Clim. Dyn., 38, 1031–1046, doi:10.1007/s00382-011-1051-z, 2012.

Le Quéré, C., Raupach, M. R., Canadell, J. G., Marland, G., Bopp, L., Ciais, P., Conway, T. J., Doney, S. C., Feely, R. A., Foster, P., Friedlingstein, P., Gurney, K., Houghton, R. A., House, J. I., Hungintford, C., Levy, P. E., Lomas, M. R., Majkut, J., Metzl, N., Ometto, J. P., Peters, G. P., Prentice, I. C., Randerson, J. T., Running, S. W., Sarmiento, J. L., Schuster, U., Sitch, S., Takahashi, T., Viovy, N., van der Werf, G. R., and Woodward, F. I.: Trends in the sources and sinks of carbon dioxide, Nature Geosci., 2, 831–836, doi:10.1038/ngeo689, 2009.

Le Quéré, C., Takahashi, T., Buitenhuis, E. T., Rödenbeck, C., and Sutherland, S. C.: Impact of climate change and variability on the global oceanic sink of CO_2, Glob. Biogeochem. Cycles, 24, GB4007, doi:10.1029/2009GB003599, 2010.

Le Quéré, C. et al.: Global carbon budget 2016, Earth Syst. Sci. Data, 8, 605–649, doi:10.5194/essd-8-605-2016, 2016.

Li, G., and Xie, S.-P.: Tropical biases in CMIP5 multimodel ensemble: The excessive equatorial pacific cold tongue and double ITCZ problems, J. Clim., 27, 1765–1780, doi:10.1175/JCLI-D-13-00337.1, 2014.

Li, H., Ilyina, T., Müller, W. A., and Sienz, F.: Decadal predictions of the North Atlantic CO_2 uptake, Nat. Commun., 7, 11076, doi:10.1038/ncomms11076, 2016.

Li, H., Ilyina, T., Müller, W. A., and Landschützer, P.: Predicting the variable ocean carbon sink. Sci. Adv. 5, eaav6471, doi: 10.1126/sciadv.aav6471, 2019.

McKinley, G. A., Follows, M. J., and Marshall, J.: Mechanisms of air–sea CO_2 flux variability in the equatorial Pacific and the North Atlantic, Glob. Biogeochem. Cycles, 18, GB2011, doi:10.1029/2003GB002179, 2004.

移動 (挿入) [8]

Mochizuki, T., Ishii, M., Kimoto, M., Chikamoto, Y., Watanabe, M., Nozawa, T., Sakamoto, T. T., Shiogama, H., Awaji, T., Sugiura, N., Toyoda, T., Yasunaka, S., Tatebe, H., and Mori, M.: Pacific decadal oscillation hindcasts relevant to near-term climate prediction, Proc. Nat. Acad. Sci. USA, 107(5), 1833–1837, doi:10.1073/pnas.0906531107, 2010.

Obata, A., and Kitamura, Y.: Interannual variability of the sea–air exchange of CO_2 from 1961 to 1998 simulated with a global ocean circulation-biogeochemistry model, J. Geophys. Res., 108(C11), 3337, doi:10.1029/2001JC001088, 2003.

Park, G.-H., Wanninkhof, R., Doney, S. C., Takahashi, T., Lee, K., Feely, R. A., Sabine, C. L., Triñanes, J., and Lima, I.: Variability of global net sea–air CO_2 fluxes over the last three decades using empirical relationships, Tellus B Chem. Phys. Meteorol., 62(5), 352–368, doi:10.1111/j.1600-0889.2010.00498.x, 2010.

Park, J.-Y., Stock, C. A., Yang, X., Dunne, J. P., Rosati, A., John, J., and Zhang, S.: Modeling global ocean biogeochemistry with physical data assimilation: A pragmatic solution to the Equatorial instability, J. Adv. Model. Earth Syst., 10, 891–906, doi:10.1002/2017MS001223, 2018.

Patra, P. K., Maksyutov, S., Ishizawa, M., Nakazawa, T., Takahashi, T., and Ukita, J.: Interannual and decadal changes in the sea–air CO_2 flux from atmospheric CO_2 inverse modeling, Glob. Biogeochem. Cycles, 19, GB4013, doi:10.1029/2004GB002257, 2005.

Pohlmann, H., Jungclaus, J. H., Köhl, A., Stammer, D., and Marotzke, J.: Initializing decadal climate predictions with the GECCO oceanic synthesis: Effects on the North Atlantic, J. Clim., 22, 3926–3938, doi:10.1175/2009JCLI2535.1, 2009.

Prather, M. J.: Numerical advection by conservation of second-order moments, J. Geophys. Res., 91, 6671–6681, 1986.

Rödenbeck, C., Bakker, D. C. E., Metzl, N., Olsen, A., Sabine, C., Cassar, N., Reum, F., Keeling, R. F., and Heimann, M.: Interannual sea–air CO_2 flux variability from an observation-driven ocean mixed-layer scheme, Biogeosciences, 11, 4599–4613, doi:10.5194/bg-11-4599-2014, 2014.

Sabine, C. L., Feely, R. A., Gruber, N., Key, R. M., Lee, K., Bullister, J. L., Wanninkhof, R., Wong, C. S., Wallace, D. W. R., Tilbrook, B., Millero, F. J., Peng, T.-H., Kozyr, A., Ono, T., and Rios, A. F.: The oceanic sink for anthropogenic CO_2, Science, 305, 367–371, doi:10.1126/science.1097403, 2004.

Sasaki, Y.: Proposed inclusion of time variation terms, observational and theoretical, in numerical variational objective analysis, J. Meteor. Soc. Japan, 47, 115–124, 1969.

Sasaki, Y.: Some basic formalisms in numerical variational analysis, Mon. Wea. Rev., 98, 875–883, 1970.

Smith, D. M., Cusack, S., Colman, A. W., Folland, C. K., Harris, G. R., and Murphy, J. M.: Improved surface temperature prediction for the coming decade from a global climate model, Science, 317, 796–799, doi:10.1126/science.1139540, 2007.

Sospedra-Alfonso, R., and Boer, G. J.: Assessing the impact of initialization on decadal prediction skill, Geophys. Res. Lett., 47, e2019GL086361. doi:1029/2019GL086361, 2020.

削除: Meehl, G. A., Gent, P. R., Arblaster, J. M., Otto-Bliesner, B. L., Brady, E. C., and Craig, A.: Factors that affect the amplitude of El Niño in global coupled climate models, Clim.

上へ移動 [8]: Clim.

削除: Dyn., 17, 515–526, doi:10.1007/PL00007929, 2001.

Sugiura, N., Awaji, T., Masuda, S., Toyoda, T., Igarashi, H., Ishikawa, Y., Ishii, M., and Kimoto, M.: Potential for decadal predictability in the North Pacific region, Geophys. Res. Lett., 36, L20701, doi:10.1029/2009GL039787, 2009.

Takahashi, T., Olafsson, J., Goddard, J. G., Chipman, D. W., and Sutherland, S. C.: Seasonal variation of CO_2 and nutrients in the high-latitude surface oceans: A comparative study, Glob. Biogeochem. Cycles, 7(4), 843–878, doi:10.1029/93GB02263, 1993.

Tatebe, H., and Hasumi, H.: Formation mechanism of the Pacific equatorial thermocline revealed by a general circulation model with a high accuracy tracer advection scheme, Ocean Modelling, 35(3), 245-252, 2010.

Tatebe, H., Ishii, M., Mochizuki, T., Chikamoto, Y., Sakamoto, T. T., Komuro, Y., Mori, M., Yasunaka, S., Watanabe, M., Ogochi, K., Suzuki, T., Nishimura, T., and Kimoto, M.: The initialization of the MIROC climate models with hydrographic data assimilation for decadal prediction, J. Meteorol. Soc. Japan, 90A, 275–294, doi:10.2151/jmsj.2012-A14, 2012.

Tatebe, H., Tanaka, Y., Komuro, Y., and Hasumi, H.: Impact of deep ocean mixing on the climatic mean state in the Southern Ocean, Sci. Rep., 8, 14479, doi: 10.1038/s41598-018-32768-6, 2018.

Taylor, K. E., Stouffer, R. J., and Meehl, G. A.: An overview of CMIP5 and the experiment design, Bull. Amer. Meteorol. Soc., 93, 485–498, doi:10.1175/BAMS-D-11-00094.1, 2012.

Tommasi, D. et al.: Managing living marine resources in a dynamic environment: The role of seasonal to decadal climate forecasts, Prog. Oceanogr., 152, 15–49, doi:10.1016/j.pocean.2016.12.011, 2017a.

Tommasi, D., Stock, C. A., Alexander, M. A., Yang, X., Rosati, A., and Vecchi, G. A.: Multi-annual climate predictions for fisheries: An assessment of skill of sea surface temperature forecasts for large marine ecosystems, Front. Mar. Sci., 4, 201, doi:10.3389/fmars.2017.00201, 2017b.

Valsala, V., and Maksyutov, S.: Simulation and assimilation of global ocean pCO_2 and air–sea CO_2 fluxes using ship observations of surface ocean pCO_2 in a simplified biogeochemical offline model, Tellus B Chem. Phys. Meteorol., 62B, 821–840, doi:10.1111/j.1600-0889.2010.00495.x, 2010.

Valsala, V., Maksyutov, S., Telszewski, M., Nakaoka, S., Nojiri, Y., Ikeda, M., and Murtugudde, R.: Climate impacts on the structures of the North Pacific air–sea CO_2 flux variability, Biogeosciences, 9, 477–492, doi:10.5194/bg-9-477-2012, 2012.

Wanninkhof, R.: Relationship between wind speed and gas exchange over the ocean, J. Geophys. Res., 97(C5), 7373–7382, doi:10.1029/92JC00188, 1992.

Wanninkhof, R.: Relationship between wind speed and gas exchange over the ocean revisited, Limnol. Oceanogr. Methods, 12, 351–362, doi:10.4319/lom.2014.12.351, 2014.

Watanabe, M., Suzuki, T., O'ishi, R., Komuro, Y., Watanabe, S., Emori, S., Takemura, T., Chikira, M., Ogura, T., Sekiguchi, M., Takata, K., Yamazaki, D., Yokohata, T., Nozawa, T., Hasumi, H., Tatebe, H., and Kimoto, M.: Improved climate simulation by MIROC5: Mean states, variability, and climate sensitivity, J. Clim., 23, 6312–6335, doi:10.1175/2010JCLI3679.1, 2010.

Watanabe, M., Chikira, M., Imada, Y., and Kimoto, M.: Convective control of ENSO simulated in MIROC, J. Clim., 24, 543–562, doi:10.1175/2010JCLI3878.1, 2011.

Watanabe, S., Hajima, T., Sudo, K., Nagashima, T., Takemura, T., Okajima, H., Nozawa, T., Kawase, H., Abe, M., Yokohata, T., Ise, T., Sato, H., Kato, E., Takata, K., Emori, S., and Kawamiya, M.: MIROC-ESM 2010: Model description and basic results of CMIP5-20c3m experiments, Geosci. Model Dev., 4, 845–872, doi:10.5194/gmd-4-845-2011, 2011.

Weiss, R.: Carbon dioxide in water and seawater: The solubility of a non-ideal gas, Mar. Chem., 2, 203–215, doi:10.1016/0304-4203(74)90015-2, 1974.

Yang, X., Rosati, A., Zhang, S., Delworth, T. L., Gudgel, R. G., Zhang, R., Vecchi, G., Anderson, W., Chang, Y.-S., DelSole, T., Dixon, K., Msadek, R., Stern, W. F., Wittenberg, A., and Zeng, F.: A predictable AMO-like pattern in the GFDL fully coupled ensemble initialization and decadal forecasting system, J. Clim., 26, 650–661, doi:10.1175/JCLI-D-12-00231.1, 2013.

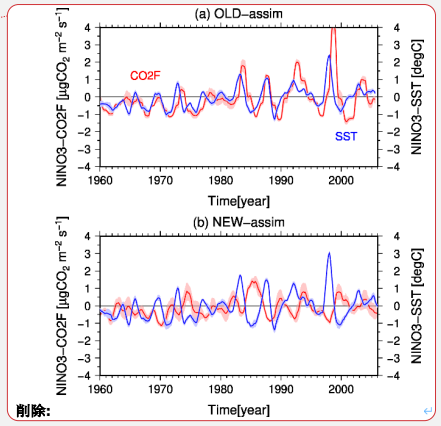

削除:

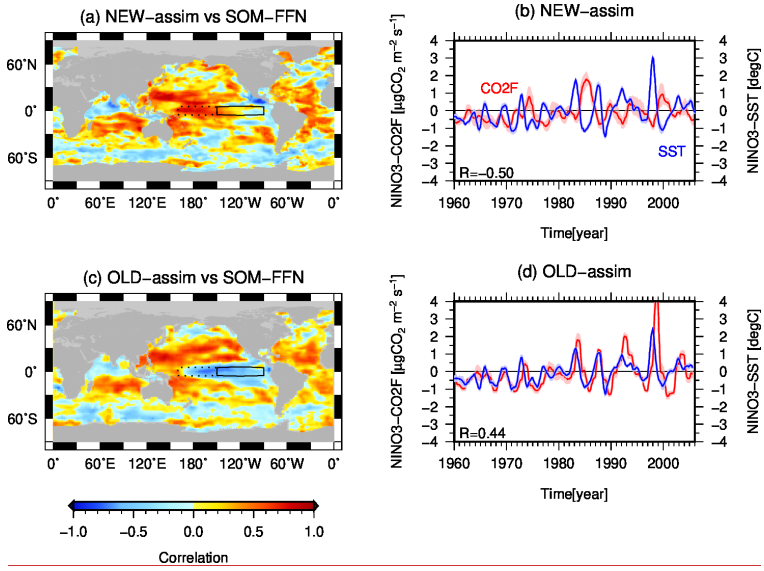

935 **Figure 1.** (a, c) Maps for correlation coefficient between monthly CO2F anomalies derived from SOM-FFN and that of (a) NEW-assim and (c) OLD-assim. The analysis period is from 1982 to 2005. The solid line boxes show Niño3 region (5°S–5°N, 90°–150°W) and the dotted line boxes show Niño4 region (5°S–5°N, 160°E–150°W). (b, d) Timeseries of the detrended NINO3-SST (blue line) and NINO3-CO2F (red line, positive upward) anomalies simulated with (b) NEW-assim and (d) OLD-assim. Values plotted are the one-year running mean, and shading in (b) and (d) shows the ensemble spread (1σ). R denotes the correlation coefficients between 940 the detrended ensemble mean NINO3-SST and NINO3-CO2F anomalies, with one-year running mean filter applied.

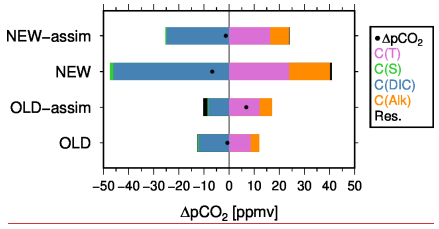

945 **Figure 2.** ΔpCO_2 (dots) and its decomposition with changes in X (X=T, S, DIC, Alk), C(X), as well as Res. (Eq. (3)) evaluated in NEW-assim, NEW, OLD-assim, and OLD.

削除: Time variations of the ensemble mean sea surface temperature (SST; blue line) and air–sea CO2 flux (CO2F, positive upward; red line) in the (a,

削除: a) OLD-assim and (

削除: standard deviation

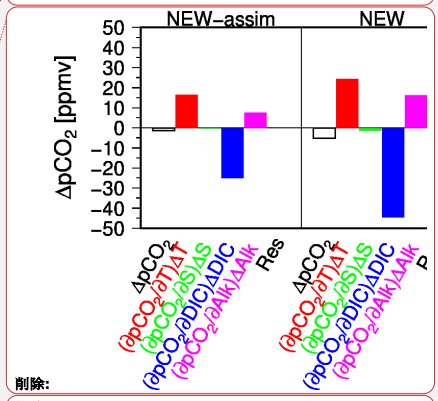

削除:

削除: Each term

削除:)

削除: ΔX (X = pCO2, T, S, DIC, or Alk) in Eq. (3) is estimated as X

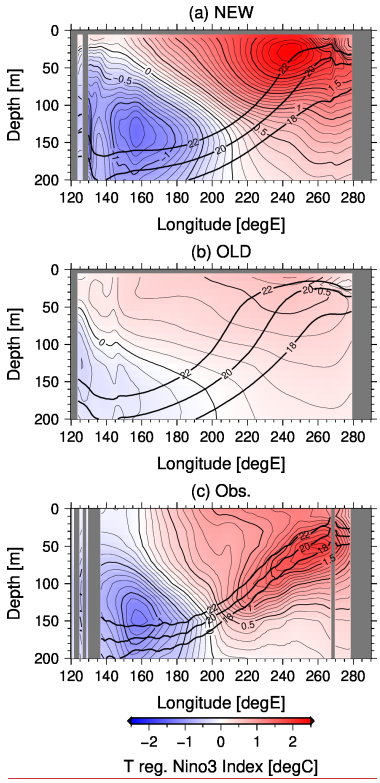

Figure 3. Anomalies of equatorial ocean temperature regressed onto NINO3-SST anomalies for NEW (top), OLD (middle), and observations (bottom). Contour interval is 0.1 °C. Thick solid lines indicates the climatological mean isotherms of the 18, 20, and 22 °C.

削除: , and ∂pCO2/∂X is estimated with the climatological annual mean T, S, DIC, and Alk at the sea surface within the Niño3 region in each model.
... [17]

削除: show

削除: annual

削除: depths

削除: isotherms

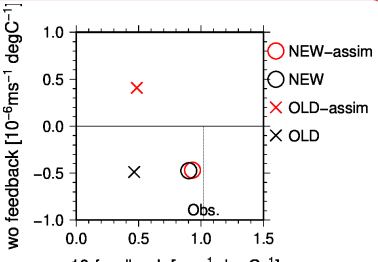

削除:

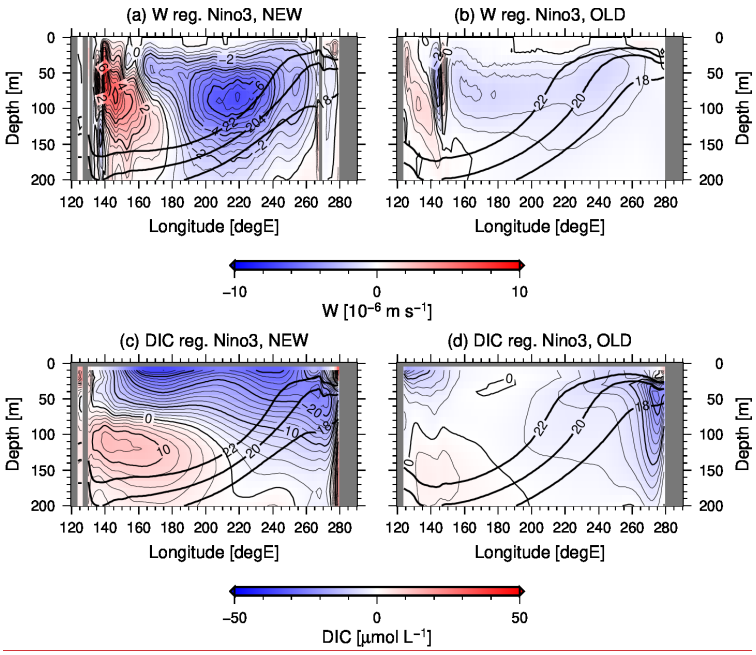

985 **Figure 4. Anomalies of equatorial vertical velocity (upper panels) and DIC (lower panels) regressed onto NINO3-SST anomalies for NEW (left) and OLD (right). Contour intervals are 0.5 × 10^{-6} m s^{-1} in (a,b) and 2 μmol L^{-1} in (c,d), respectively. Thick solid lines indicates the climatological-mean isotherms of the 18, 20, and 22 °C.**

削除: Relationship between the wind (u10) feedback and the

削除: wo) feedback in OLD (black cross), OLD-assim (red cross), NEW (black circle), and NEW-assim (red circle). Wind feedback (vertical velocity feedback) was computed as the regression of NINO4-U10 over NINO3-SST (m s−1 °C−1) (regression of NINO3-WO over NINO3-SST (m s−1 °C−1)). Thin dashed line shows wind feedback evaluated from the JRA55 reanalysis wind dataset (Kobayashi et al., 2015) and the COBESST2 dataset (Ishii et al., 2005; Hirahara et al., 2014).

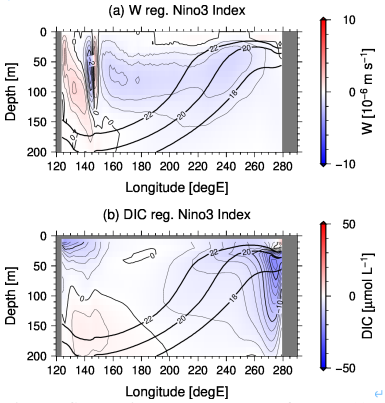

Figure 5. Cross sections along the Equator of monthly (a) upward velocity upper panels)

削除: (b) DIC concentration anomalies with OLD, each

削除: .

削除: interval is

書式を変更: 上付き

削除: b).

書式を変更: 上付き

書式を変更: 上付き

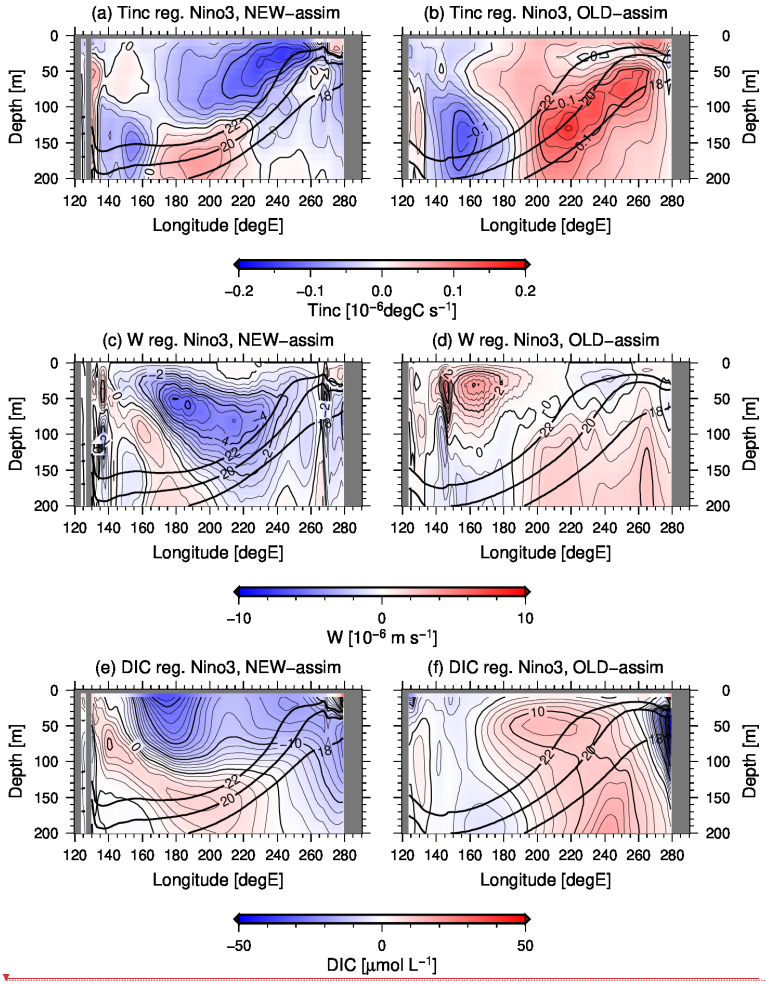

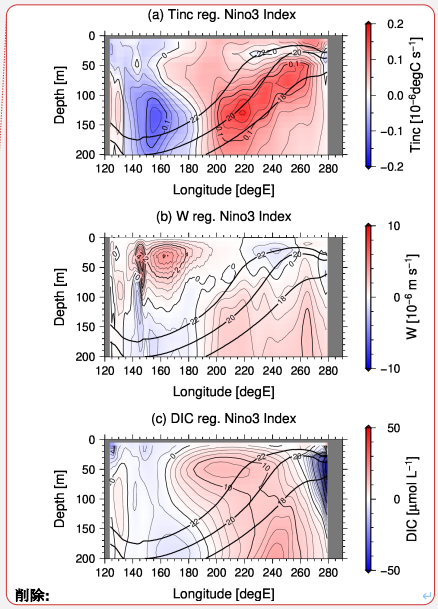

Figure 5. Equatorial temperature analysis increments (top panels), vertical velocity anomalies (middle panels) and DIC anomalies (bottom panels) regressed onto NINO3-SST anomalies for NEW-assim (left) and OLD-assim (right). Contour intervals are 0.02 × 10^{-6} °C s^{-1} in (a,b), 0.5 × 10^{-6} m s^{-1} in (c,d) and 2 µmol L^{-1} in (e,f), respectively. Thick solid lines indicates the climatological-mean isotherms of the 18, 20, and 22 °C.

削除: 6. Cross sections along the Equator of (a) water
削除: increment, (b) upward
削除: ,
削除: (c)
削除: concentration with OLD-assim each
削除: .
削除: interval is
削除: b),
削除: c).

Table 1. Correlation coefficients between detrended one-year running mean NINO3-SST and NINO3-CO2F anomalies in NEW-assim, NEW, OLD-assim, OLD, and observations. The correlations coefficients in NEW-assim, NEW, OLD-assim, and OLD are for the period from 1961 to 2005 (Figures 1 and S2), and that in observations are for the period from 1982 to 2005.

	NEW-assim	NEW	OLD-assim	OLD	Observation
Corr. Coeff.	–0.50	–0.85	0.44	–0.67	–0.75

Table 2. The intensity and period of ENSO in NEW, OLD, and observations calculated from the one-year running mean NINO3-SST anomalies for the period from 1961 to 2005.

	NEW	OLD	Observation
Intensity of ENSO [°C]	1.17	0.43	0.80
Period of ENSO [yr]	5.0	4.5	3.5

Table 3. The wind feedback computed as the monthly 10 m zonal wind anomalies in the Niño4 region which is regressed onto the monthly NINO3-SST anomalies and the vertical velocity feedback computed as the monthly vertical velocity anomalies at the depth of the 20 °C isotherm in the Niño3 region which is regressed onto the monthly NINO3-SST anomalies in NEW-assim, NEW, OLD, and OLD-assim. The wind feedback is also evaluated from the observation dataset.

	NEW-assim	NEW	OLD-assim	OLD	Observation
Wind feedback [m s^{-1} K^{-1}]	0.92	0.92	0.48	0.46	1.02
Vertical velocity feedback [m s^{-1} K^{-1}]	-4.5×10^{-7}	-3.9×10^{-7}	4.1×10^{-7}	-4.9×10^{-7}	N/A

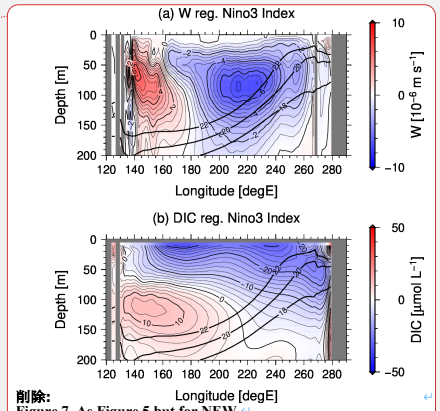

削除:
Figure 7. As Figure 5 but for NEW.

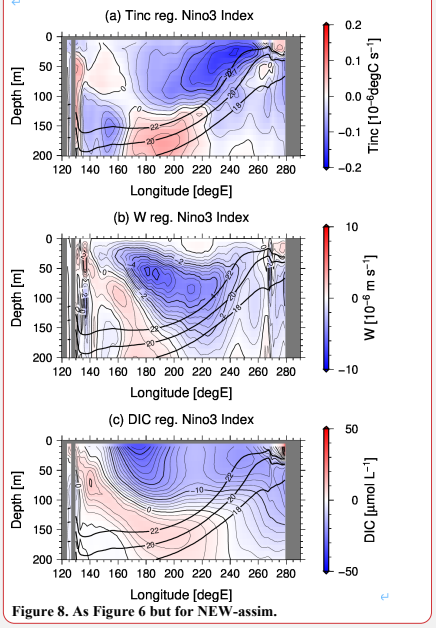

Figure 8. As Figure 6 but for NEW-assim.